



Paleoceanography

RESEARCH ARTICLE

10.1002/2014PA002656

Key Points:

- Oligocene productivity was lower than in Eocene and modern times
- Barite, benthic foraminifera proxies appear antithetical to opal and diatoms
- The thermocline appears to have been deep in the earliest Oligocene

Supporting Information:

- Readme
- Figure S1
- Figure S2
- Figure S3
- Table S1
- Table S2
- Table S3
- Table S4

Correspondence to:

T. C. Moore Jr.,
tedmoore@umich.edu

Citation:

Moore, T. C., Jr., B. S. Wade, T. Westerhold, A. M. Erhardt, H. K. Coxall, J. Baldauf, and M. Wagner (2014), Equatorial Pacific productivity changes near the Eocene-Oligocene boundary, *Paleoceanography*, 29, doi:10.1002/2014PA002656.

Received 7 APR 2014

Accepted 6 AUG 2014

Accepted article online 12 AUG 2014

Equatorial Pacific productivity changes near the Eocene-Oligocene boundary

T. C. Moore Jr.¹, Bridget S. Wade², Thomas Westerhold³, Andrea M. Erhardt⁴, Helen K. Coxall⁵, Jack Baldauf⁶, and Meghan Wagner⁷

¹Department of Earth and Environmental Sciences, University of Michigan, Ann Arbor, Michigan, USA, ²Department of Earth Sciences, University College London, London, UK, ³MARUM, University of Bremen, Bremen, Germany, ⁴Department of Earth Sciences, University of Cambridge, Cambridge, UK, ⁵Department of Geological Sciences, Stockholm University, Stockholm, Sweden, ⁶Department of Geosciences, Texas A&M University, College Station, Texas, USA, ⁷Department of Earth and Atmospheric Sciences, Central Michigan University, Mount Pleasant, Michigan, USA

Abstract There is general agreement that productivity in high latitudes increased in the late Eocene and remained high in the early Oligocene. Evidence for both increased and decreased productivity across the Eocene-Oligocene transition (EOT) in the tropics has been presented, usually based on only one paleoproductivity proxy and often in sites with incomplete recovery of the EOT itself. A complete record of the Eocene-Oligocene transition was obtained at three drill sites in the eastern equatorial Pacific Ocean (ODP Site 1218 and IODP Sites U1333 and U1334). Four paleoproductivity proxies that have been examined at these sites, together with carbon and oxygen isotope measurements on early Oligocene planktonic foraminifera, give evidence of ecologic and oceanographic change across this climatically important boundary. Export productivity dropped sharply in the basal Oligocene (~33.7 Ma) and only recovered several hundred thousand years later; however, overall paleoproductivity in the early Oligocene never reached the average levels found in the late Eocene and in more modern times. Changes in the isotopic gradients between deep- and shallow-living planktonic foraminifera suggest a gradual shoaling of the thermocline through the early Oligocene that, on average, affected accumulation rates of barite, benthic foraminifera, and opal, as well as diatom abundance near 33.5 Ma. An interval with abundant large diatoms beginning at 33.3 Ma suggests an intermediate thermocline depth, which was followed by further shoaling, a dominance of smaller diatoms, and an increase in average primary productivity as estimated from accumulation rates of benthic foraminifera.

1. Introduction

As the world passed from the warm Eocene into the colder Oligocene, there were profound changes in the ecology, productivity, chemistry, and presumably the vertical structure of the tropical Pacific water column. This major shift in climatic state is evidenced by step-like changes in the oxygen and carbon isotopes of deep-sea benthic foraminifera [Coxall *et al.*, 2005; Coxall and Wilson, 2011] as well as in the lithology of pelagic sediments [Pälike *et al.*, 2012, and references therein] that mirrored the cooling of the oceans as a whole and the development of large ice sheets on Antarctica [Kennett and Shackleton, 1976; Zachos *et al.*, 1996; DeConto and Pollard, 2003; Coxall *et al.*, 2005; Lear *et al.*, 2008]. There were also increased weathering on land [e.g., Lear *et al.*, 2003; Pälike *et al.*, 2012; Misra and Froelich, 2012], and the depletion of labile carbon and other nutrients in the deep ocean that had built up in the “hot house” world [Olivarez Lyle and Lyle, 2006a, 2006b; Pälike *et al.*, 2012]. These climatic changes were associated with a drawdown of atmospheric carbon dioxide [Pearson *et al.*, 2009; Pagani *et al.*, 2011], extinction of many phytoplankton and zooplankton species [e.g., Funakawa *et al.*, 2006; Pearson *et al.*, 2008], and with tectonic changes that opened gateways to oceanic flow around Antarctica [e.g., Exon *et al.*, 2004; Stickley *et al.*, 2004; Barker *et al.*, 2007].

In the tropical Pacific, the Eocene-Oligocene transition (EOT, ~34 Ma–~33.7 Ma) [Westerhold *et al.*, 2014] is marked not only by a sharp drop in the calcite compensation depth (CCD) [van Andel, 1975; Coxall *et al.*, 2005; Pälike *et al.*, 2012] but it is also the time when the radiolarians, a heterotrophic zooplankton, are supplanted by diatoms as the major contributor of biogenic opal to the deep-sea floor [Cervato and Burckle, 2003; Lazarus *et al.*, 2009]. Radiolarian tests dominate the siliceous ooze of the tropical Pacific in the middle and upper Eocene and in concert with their common photosymbionts were likely major contributors to the overall productivity of the equatorial

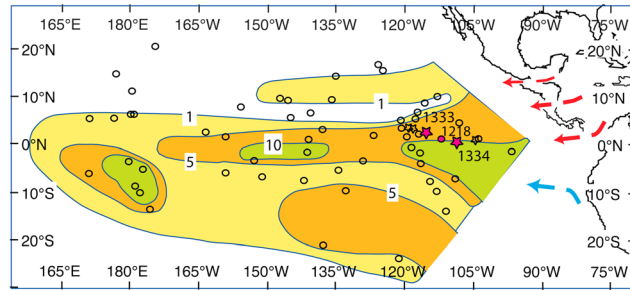


Figure 1. Map of sediment accumulation rates (m/Myr) in the tropical Pacific at 32 Ma (averaged from 30 Ma to 34 Ma [from Moore *et al.*, 2004]). Site locations from original map adjusted according to Parés and Moore [2005]. Circles denote site locations used in original work; stars indicate sites from IODP Expedition 320. Filled symbols and labels denote the three sites used in this study. Arrows indicate likely flow of surface waters with warm tropical waters (red) flowing from the Atlantic to the Pacific through the Panamanian Seaway and colder water (blue) advected into the equatorial region from the southwest via the eastern boundary current.

Pacific during these times. However, the EOT is associated with a large turnover in the radiolarian assemblage [Funakawa *et al.*, 2006] as well as a marked drop in the average silicification of radiolarian tests [Lazarus *et al.*, 2009].

Diatoms, one of the most important pelagic phytoplankton groups in the modern ocean, only came to be important in the tropical Pacific beginning in the gradual cooling phase of the late Eocene and did not fully blossom into a diverse flora, as they are today in the tropical and North Pacific, until the Oligocene [Cervato and Burckle, 2003; Rabosky and Sorhannus, 2009]. The rather late entrance of common diatoms into the open ocean tropics led Cervato

and Burckle [2003] to speculate that tropical productivity had been rather low in earlier times. However, later work [Schumacher and Lazarus, 2004] shows no increase in export productivity in the tropical Oligocene, and in fact, some studies [Griffith *et al.*, 2010; Erhardt *et al.*, 2013] indicate that export productivity was relatively high in the tropics in the late and late middle Eocene but dropped sharply at Oi-1 in the earliest Oligocene, while in high latitudes export productivity was high in the late Eocene and continued to be high in the early Oligocene [e.g., Diester-Haass and Zahn, 1996; Salamy and Zachos, 1999; Plancaq *et al.*, 2014]. However, Coxall and Wilson [2011] state that the accumulation rate of benthic foraminifera in the tropical Pacific (Site 1218) suggests that there was a high-to-low-latitude coupling in productivity and carbon sequestration.

There have been several proxies proposed as useful indices of oceanic export productivity, including diatom abundance, P/Ti ratios, and excess phosphorous, as well as accumulation rates of total organic carbon, barite, benthic foraminifera, and biogenic opal [e.g., Diester-Haass, 1995; Salamy and Zachos, 1999; Loubere, 1994; Latimer and Filippelli, 2002; Anderson and Delaney, 2005; Faul and Delaney, 2010]. All these proxies are subject to effects other than primary productivity. If two or more such proxies agree, we might feel more confident that they are giving us a credible index of past productivity and if they do not, why might they be giving us different signals?

In this study we look at three sites drilled in the tropical Pacific that contain what we believe are complete records across the Eocene-Oligocene (E/O) boundary (ODP Site 1218 and IODP Sites U1333 and U1334; Figure 1). We address the following questions: (1) what was the true change in paleoproductivity as we passed from the warm Eocene times to the cooler Oligocene, (2) what is the significance of the observed changes in the diatom and radiolarian assemblages in terms of the ecology and overall productivity of the tropics, and (3) can we deduce how the observed changes in the productivity proxies might be related to oceanographic changes in the deep and shallow waters of the tropical Pacific? We focus on the late Eocene to early Oligocene interval, extending from 36 Ma to ~31 Ma. This spans the cool down from the middle to late Eocene climatic optimum [Bohaty and Zachos, 2003], the EOT, the marked decrease in the silicification of radiolarians (35 Ma–33 Ma) [Lazarus *et al.*, 2009], and the Oi-1a and Oi-1b glacial events at the base of the Oligocene and extends through the blossoming of both large and small diatoms during the early Oligocene. We evaluate three proxies for export productivity (accumulation rates of barite and opal, as well as diatom abundance), as these proxies rapidly changed near and just above the end of the Eocene. In addition, we use the empirical relation between benthic foraminifera accumulation rates and primary productivity (as opposed to “export productivity”) [Herguera and Berger, 1991] to compare with other proxies in the Oligocene section. We also examine data on the near-surface structure of the water column as revealed by measures of $\delta^{18}\text{O}$ and $\delta^{13}\text{C}$ in deep- and shallow-living planktonic foraminifera. This information can then be compared with changes in proxies of past productivity. Combining such isotopic proxies of upper water structure with several proxies for paleoproductivity has rarely been done.

1.1. Paleoproductivity Proxies

1.1.1. BAR

Barite is formed and is preserved in deeper waters where dissolved nutrients are high, with the highest concentrations of particulate barite found in the region of the oxygen minimum zone [Paytan and Griffith, 2007]. Sediment trap studies show that the flux of biogenic barite (i.e., barite in excess of terrigenous supply) is directly related to the flux of organic carbon [Dymond *et al.*, 1992; Eagle *et al.*, 2003]; thus, barite accumulation rates in pelagic sediments are thought to be a good proxy for export productivity [e.g., Erhardt *et al.*, 2013, and references therein]. However, there are a few caveats to the use of barite as a paleoproductivity proxy that pertain to preservation in anoxic sections [Torres *et al.*, 1996] and precipitation in hydrothermal settings [e.g., Feely *et al.*, 1987, 1990]. Neither anoxic nor hydrothermal sediments are found in the upper Eocene or lower Oligocene of Site U1333 in which the barite accumulation rates used here were measured (Figure 1) [Erhardt *et al.*, 2013]. However, the degree of saturation of barium in the deep and bottom waters can also affect barite formation and preservation [Paytan and Griffith, 2007], and thus, variation in barite accumulation rates can be affected by variation in the barite saturation of deep and bottom waters at a site. Data for barite accumulation rates (BAR) used herein are adjusted to a new time scale [Westerhold *et al.*, 2014] and given in Table S1 in the supporting information. This new time scale makes substantial changes in the character of the BAR curve in the uppermost Eocene [cf. Erhardt *et al.*, 2013].

1.1.2. BFAR

Several studies report that the accumulation rate of benthic foraminifera can be related to the flux of particulate organic carbon from overlying waters [Gooday and Rathburn, 1999; Herguera, 2000; Hayward *et al.*, 2002], as can the assemblage of benthic foraminifera found in the underlying sediment [Loubere, 1994; Fariduddin and Loubere, 1997; Van der Zwaan *et al.*, 1999; Loubere, 2002]. Another factor that has been shown to be important to the abundance and species makeup of the benthic foraminifera is the degree of oxygenation of bottom waters [Loubere, 1994; Fariduddin and Loubere, 1997; Van der Zwaan *et al.*, 1999]. Finally, there is a third environmental factor, which is less well documented. This is the degree of turbulence or average bottom current speed at a given site [Aller, 1997; Gooday and Rathburn, 1999; Hayward *et al.*, 2002]. While strong boundary currents can cause erosion and a diminution of the benthic community [Herguera and Berger, 1991], moderate current velocities (≤ 15 cm/s) may enhance transport of particulate organic carbon over a site and enhance the oxygenation of waters above a site [Levin and Thomas, 1989; Gooday, 1994; Aller, 1997; Hayward *et al.*, 2002].

There are a few things that might disturb the accuracy of this proxy; chief among them is the degree of preservation of calcium carbonate, from which many deep-sea benthic foraminifera build their tests. Dissolution of carbonate strongly impacts the Eocene record studied here because of the shallow CCD during this interval. Only the Oligocene record used herein contains well-preserved carbonate that can be used in the study of foraminifera. In addition, water depth influences the amount of organic material that actually reaches the bottom; however, this factor has been incorporated in the empirical conversion of measured Benthic Foraminifera Accumulation Rates (BFAR) to the estimation of primary productivity [Herguera and Berger, 1991] that is used here (Table S2).

1.1.3. Opal Accumulation Rates and Diatom Abundance

Biogenic opal preserved in deep-sea sediments is derived mainly from diatoms and radiolarians. Diatoms are rare in the Eocene; thus, the opal accumulation in this part of the record is dominated by the radiolarians [Moore *et al.*, 2008]. Abundant diatoms in the pelagic realm are usually associated with high nutrient content of upwelled waters and high primary productivity. Coccolithophorids, the other important planktonic algae whose carbonate platelets are preserved in the sediments, are better adapted to lower nutrient levels [Lisitzin, 1972; Egge and Aksnes, 1992]. In the region of equatorial divergence in the modern eastern tropical Pacific, the band of rapidly accumulating carbonate-rich sediments (dominated by coccoliths) stretches from 6°N to 4°S, whereas the equatorial band of sediments with relatively high opal content spans only 2°N to 4°S [Weber and Pisias, 1999]. Using opal accumulation rates as a proxy for export productivity through time does have some dangers. It supposes that variation in opal accumulation signifies variation in the strength and/or duration of upwelling, assuming that neither the nutrient richness of the upwelled waters nor the preservation of the biogenic opal on the sea floor changes with time. Both of these factors could change over the time interval studied here. Opal preservation in the sites used here (Site 1218 and Site U1334) is poor to moderate for diatoms and moderate to good for radiolarians with no strong cyclic variation in these estimates [Moore and Kamikuri, 2012; Baldauf, 2013].

Upwelling systems are usually highly seasonal, with additional interannual to decadal variability; thus, on short time scales opal accumulation rate and diatom abundance do not give an integrated annual measure of total primary productivity. Even so, some studies of the equatorial Pacific show a high degree of correlation between opal accumulation rates and barite accumulation rates over the last 1 Myr [e.g., Murray *et al.*, 2012] where the greater time scale produces a natural averaging. Diatom abundance measured in the noncarbonate fraction of Site U1334 [Baldauf, 2013] provides a good check on opal accumulation rates in the Oligocene part of the section. Estimates of diatom abundance suffer from the same problems as opal accumulation rates as indicators of export productivity, especially variation in preservation on the seafloor.

2. Materials and Methods

2.1. Sites Studied

We focus our efforts on the only three sites in the tropical Pacific that appear to have recovered a complete record of the EOT: ODP Site 1218 and IODP Sites U1333 and U1334 (Figure 1). The work of Westerhold *et al.* [2012] greatly facilitated this study by providing a revised depth scale for all holes at a group of tropical Pacific sites, including IODP Sites U1331, U1332, U1333, and U1334 and ODP Sites 1218, 1219, and 1220. This allowed samples from any given hole to be placed in relative stratigraphic order with respect to samples from all other holes at each site. This depth adjustment was based on a decimeter-scale correlation using multisensor track data of all cores at each of the sites covered in their study. In a further refinement that is critical to sites used in this study, Sites U1333 and U1334 were correlated to Site 1218 using the same correlation techniques. This has allowed us to place all samples used in this study on a common (Site 1218) depth scale, thus greatly enhancing our ability to refine our stratigraphy in these three sites and to correlate accurately data from all sites studied [Westerhold *et al.*, 2012]. In this paper all depths are given in corrected revised meters composite depth (rmcd) in Site 1218.

Sites 1218 and U1334 were within $\sim 2^\circ$ of the equator during the early Oligocene; Site U1333 was slightly farther north at about 3°N (Figure 1) [Moore and Kamikuri, 2012, Table 1]. Barium accumulation rates were determined in Site U1333 [Erhardt *et al.*, 2013]; diatom abundance and assemblage data [Baldauf, 2013] and planktonic foraminiferal isotopic data presented here come from Site U1334. Opal accumulation rates used in this study were measured in Site 1218 and are taken from Lyle *et al.* [2005], Vanden Berg and Jarrard [2004], and Moore *et al.* [2008], together with a modest amount of new data measured using the technique described in Olivarez Lyle and Lyle [2002] (data in Table S3). Diatom/Radiolarian ratios in the coarse fraction ($>63\ \mu\text{m}$) were determined in all three sites.

2.2. Time Scale

We use the most recent revision of the time scale for the late Eocene and early Oligocene [Westerhold *et al.*, 2014]. We use this time scale to correct the estimates of accumulation rates of barite [Erhardt *et al.*, 2013], opal [Lyle *et al.*, 2005; Vanden Berg and Jarrard, 2004; Moore *et al.*, 2008], and benthic foraminifera [Coxall and Wilson, 2011] (see Tables S1–S3).

2.3. Diatom Assemblage

A total of 312 samples were examined from the composite sequence of Site U1334. Diatoms were analyzed using a subsample of the residue of acidified (with HCl and H_2O_2) sediment that was placed on cover slips, dried and mounted in Hyrax on $22 \times 75\ \text{mm}$ glass slides [Baldauf, 2013]. The counting techniques of Schrader and Gersonde [1978] were utilized for all samples. Diatom, silicoflagellate, and radiolarian specimens observed in the first 100 fields of view were tabulated. The total number of diatoms was not tabulated for the few samples where diatoms were rare or absent. See the data report of Baldauf [2013] for data tables and estimates of fragmentation and preservation.

2.4. Diatom/Radiolarian Ratio in the $>63\ \mu\text{m}$ Fraction

Based on the correlation of multisensor track data and paleomagnetic stratigraphy, 1 cm samples (one quarter core) were taken over the stratigraphic interval spanning from $\sim 40\ \text{Ma}$ to $\sim 30\ \text{Ma}$ in the three sites studied [Moore and Kamikuri, 2012]. Sample spacing varied between $\sim 20\ \text{cm}$ and $50\ \text{cm}$, with an average sample spacing in the sites of $\sim 35\ \text{cm}$.

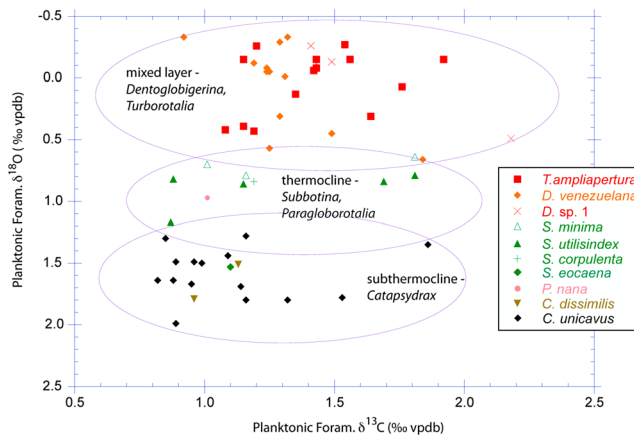


Figure 2. Carbon versus oxygen isotopes for ten planktonic foraminiferal species from the lower Oligocene of Site U1334. *D. sp. 1* = *Dentoglobigerina sp. 1* (see text).

Details of the radiolarian sample preparation and data tables of radiolarian species counts, preservation, and D/R ratios in the samples are given in the data report of Moore and Kamikuri [2012].

2.5. Planktonic Foraminiferal Isotopic Measurements

Stable isotope measurements ($\delta^{18}\text{O}$, $\delta^{13}\text{C}$) were conducted on multiple species of planktonic foraminifera from the lowermost Oligocene of Hole U1334A. Planktonic foraminifera are usually poorly preserved or absent in the Eocene section, and in the Oligocene section preservation is moderate to poor. All specimens are recrystallized. Specimens with infilling and overgrowth were avoided.

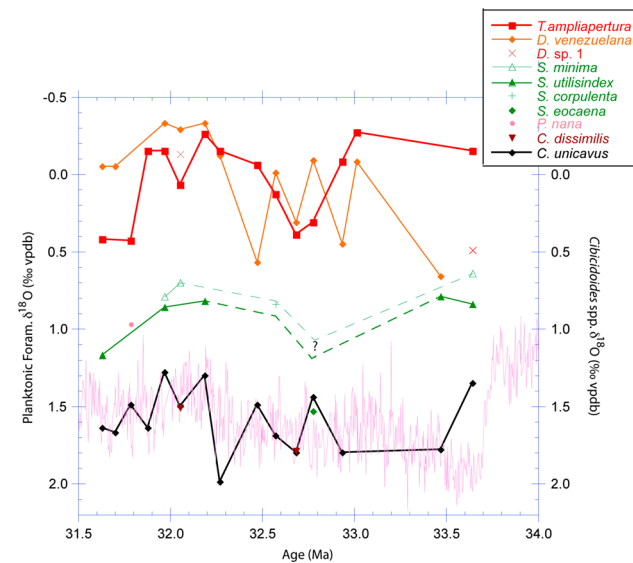


Figure 3. Oxygen isotopic data from Site U1334 plotted versus age (Ma). Red line and symbols indicate mixed-layer species *Turborotalia ampliapertura*; orange line and symbols represent mixed-layer species *Dentoglobigerina venezuelana*. Light green line with open symbols and dark green line with filled symbols indicate thermocline species *Subbotina minima* and *S. utilisindex*, respectively. Dashed green lines indicate possible values of thermocline $\delta^{18}\text{O}$ based on other species of *Subbotina* (*S. corpulenta* and *S. eocaena*). Black line and symbols indicate subthermocline species *Catapsydrax unicavus* (cf. Figure 2). Light purple line indicates benthic foraminifera (*Cibicidoides* spp.) $\delta^{18}\text{O}$ from Site 1218 [Coxall and Wilson, 2011].

Samples for the study of the siliceous coarse fraction ($>63\ \mu\text{m}$) were prepared following the procedures described in Moore and Kamikuri [2012]. The area scanned on each slide was adjusted to assure that ~ 5000 to 10,000 radiolarian specimens were examined. In establishing the Diatom/Radiolarian (D/R) ratio, the portion of a fragmented radiolarian test had to be identifiable at least at the genus level to be counted. This usually meant that at least half the main part of the test was preserved. Smaller fragments were not counted. All diatom valve fragments greater than one half the original valve were counted, as were all diatom girdles.

Specimens were analyzed every 1.5 m between 216 and 244 m below seafloor in Hole U1334A (Samples U1334A-24X-2, 43–45 cm to U1334A-27X-1 43–45 cm, equivalent to 212.9 rmcd to 237.9 rmcd in Site 1218). *Turborotalia ampliapertura*, *Dentoglobigerina venezuelana*, and *Catapsydrax unicavus* were abundant and picked for most samples. In addition, *Subbotina utilisindex*, *S. minima*, *S. corpulenta*, *S. eocaena*, *Paragloborotalia nana*, *C. dissimilis*, and *Dentoglobigerina sp. 1* [see Wade and Pearson, 2008] were picked when available. Stable isotope analyses were conducted at the University of Michigan. Replicate analysis of NBS-19 standards yielded a standard deviation of 0.04‰ and 0.03‰ for $\delta^{18}\text{O}$ and $\delta^{13}\text{C}$, respectively. Isotopic data are listed in Table S4.

3. Results

3.1. Planktonic Foraminiferal Oxygen and Carbon Isotopes

Despite the diagenetic alteration of the planktonic foraminifera specimens,

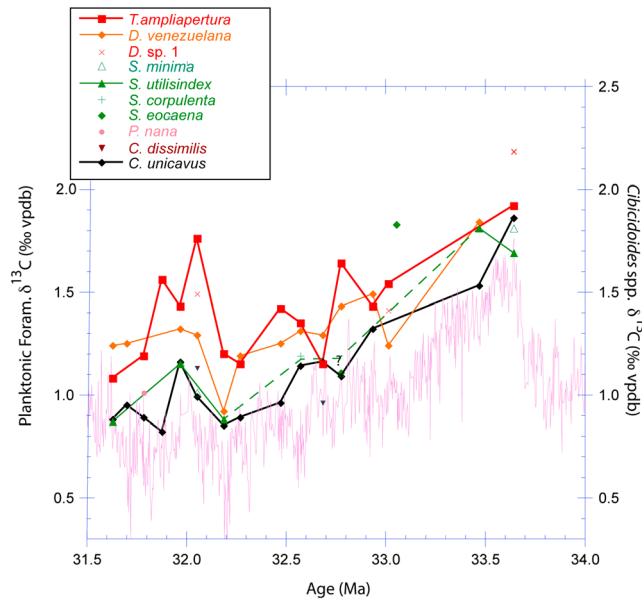


Figure 4. Carbon isotopic data from Site U1334 plotted versus age (Ma). Red line and symbols indicate mixed-layer species *Turborotalia ampliapertura*; orange line and symbols represent mixed-layer species *Dentoglobigerina venezuelana*. Green line with filled symbols indicates thermocline species *Subbotina utilisindex*. Dashed green line indicates possible values of thermocline $\delta^{13}\text{C}$ based on other species of *Subbotina* (*S. corpulenta* and *S. eoacaena*). Black line and symbols indicate subthermocline species *Catapsydrax unicavus* (cf. Figure 2). Light purple line indicates benthic foraminifera (*Cibicidoides* spp.) $\delta^{13}\text{C}$ from Site 1218 [Coxall and Wilson, 2011].

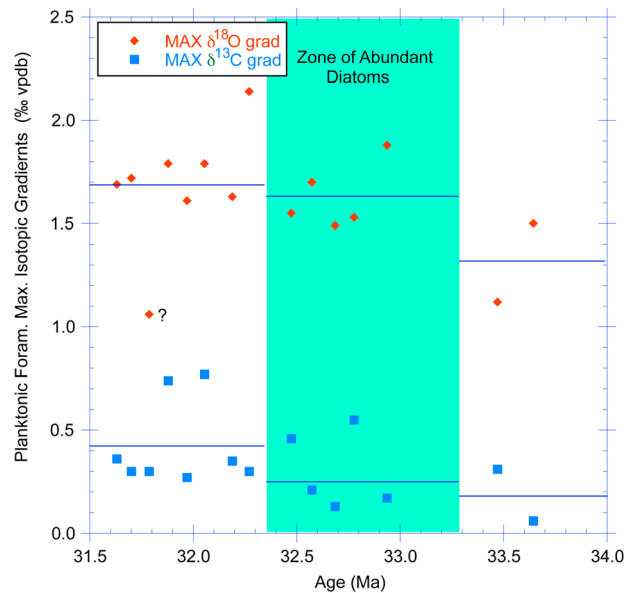


Figure 5. Maximum isotopic gradient between subthermocline species (*Catapsydrax unicavus*) and mixed-layer species (*Turborotalia ampliapertura* or *Dentoglobigerina venezuelana*) plotted versus age (Ma) (cf. Figures 3 and 4). Blue squares indicate carbon isotope gradients; orange diamonds indicate oxygen isotope gradients. Zone of abundant diatoms (green rectangle) (cf. Figures 6 and 7). Horizontal lines denote average values within each age interval.

stable isotope data indicate a $\delta^{18}\text{O}$ gradient of 2.3‰ between the subthermocline and mixed-layer species, offsets consistent with previous studies [e.g., Poore and Matthews, 1984; Grant and Dickens, 2002; Wade et al., 2007; Wade and Pearson, 2008; Faul and Delaney, 2010] (Figures 2–5).

Oxygen isotope results indicate a well-stratified water column in the early Oligocene at Site U1334 over the interval studied (Figure 3). Mixed-layer species *T. ampliapertura* and *D. venezuelana* fluctuate by approximately 1‰ between -0.33‰ and 0.64‰ . Their isotopic-depth ordering shows more variation than is seen among the thermocline and subthermocline dwellers.

Subbotina minima, *S. utilisindex*, *S. corpulenta*, and perhaps *S. eoacaena* are thought to live near the thermocline with $\delta^{18}\text{O}$ values that are generally intermediate between the mixed-layer species and the subthermocline species, *Catapsydrax unicavus*. *Subbotina minima* records slightly more negative $\delta^{18}\text{O}$ values in comparison to *S. utilisindex*. A single sample of *S. eoacaena* has values of both carbon and oxygen isotopes similar to that of *Catapsydrax unicavus*, and *C. unicavus* records $\delta^{18}\text{O}$ values similar to those of benthic foraminifera (Figure 3). *C. dissimilis* was analyzed from two samples and records nearly identical $\delta^{18}\text{O}$ values to *C. unicavus*.

Planktonic foraminiferal $\delta^{13}\text{C}$ values decrease through the studied section from 1.9 to 1.0‰ following the $\delta^{13}\text{C}$ maxima in the earliest Oligocene (Figure 4). The gradient between planktonic and benthic foraminiferal $\delta^{13}\text{C}$ values is low, generally $<0.5\text{‰}$ compared to a typical vertical $\delta^{13}\text{C}$ profile seen in the modern ocean at this latitude ($\sim 1.0\text{‰}$) or a well-stratified region of the Pacific (2.0‰) [Kroopnick, 1985]. The $\delta^{13}\text{C}$ profile is consistent with the $\delta^{18}\text{O}$ depth ordering, with *T. ampliapertura* and dentoglobigerinids exhibiting the most positive $\delta^{13}\text{C}$ values indicative of the surface mixed layer.

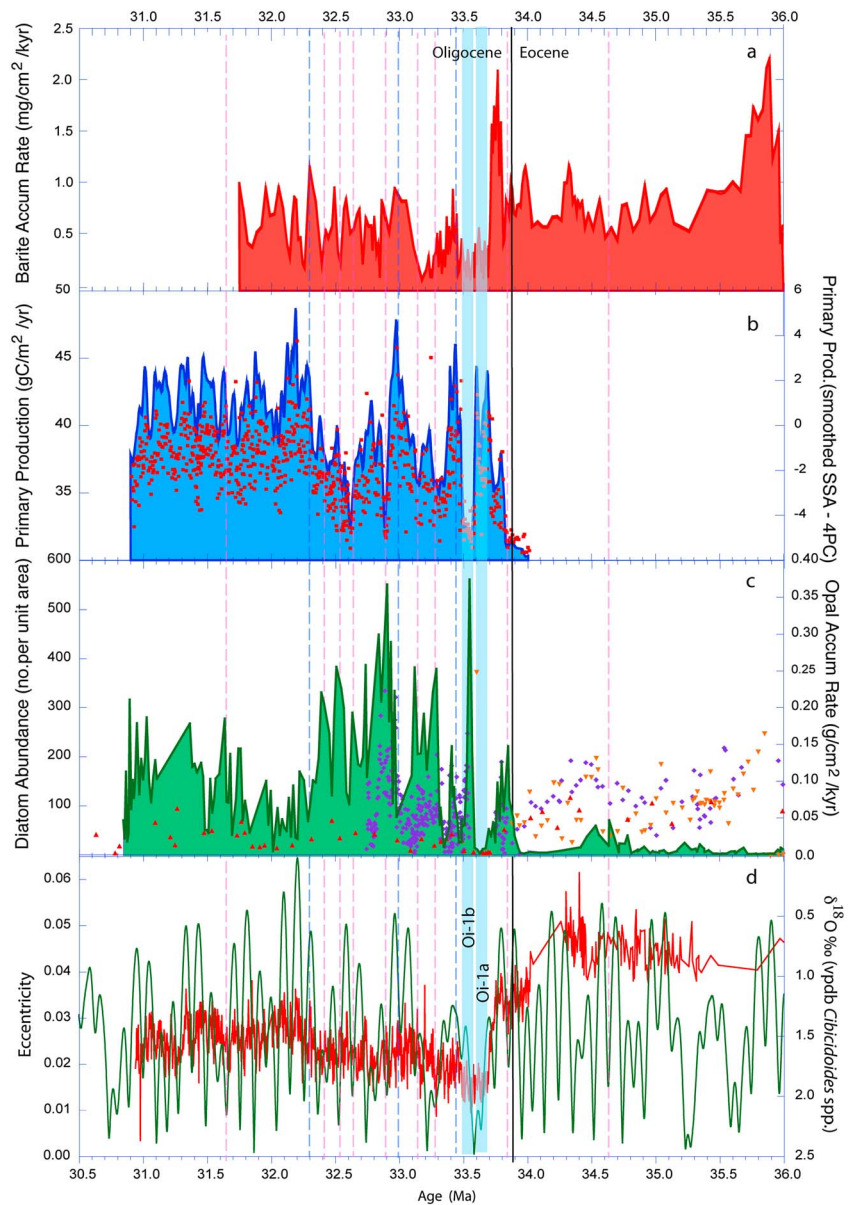


Figure 6. Proxy measurements for paleoproductivity. (a) Barite accumulation rates, proxy for export productivity measured in Site U1333 (corrected from *Erhardt et al.* [2013]): red-filled curve. (b) Blue curve and red squares, estimates of primary productivity [*Herguera and Berger*, 1991] based on benthic foraminifera (>150 μm) accumulation rate in Site 1218 (corrected from *Coxall and Wilson* [2011]). Red squares are individual sample estimates (see Table S2). Blue curve, sample data smoothed using single spectrum analysis [*Paillard et al.*, 1996] with four principal components. (c) Diatom abundance measured in 100 fields of view (see text) on strewn (settled) slide samples, proxy for export productivity from Site U1334 [*Baldauf*, 2013]: green-filled curve. Opal accumulation rates measured in Site 1218, proxy for export productivity: blue triangles from *Vanden Berg and Jarrard* [2004] as adjusted by *Moore et al.* [2008], orange inverted triangles from *Lyle et al.* [2005], and red triangles from this study. (d) Red curve: oxygen isotopes measured on benthic foraminifera [*Coxall and Wilson*, 2011]; green curve: orbital eccentricity [*Laskar et al.*, 2011]. Vertical dashed lines illustrate positive relationship between BAR, primary productivity, and high eccentricity (blue) and positive relationship between diatom abundance, opal MAR, and low eccentricity (red). All data plotted versus age (Ma) [*Westerhold et al.*, 2014]. Light blue vertical bars indicate glacial intervals Oi-1a and Oi-1b. Vertical black line indicates Eocene-Oligocene boundary [*Westerhold et al.*, 2014].

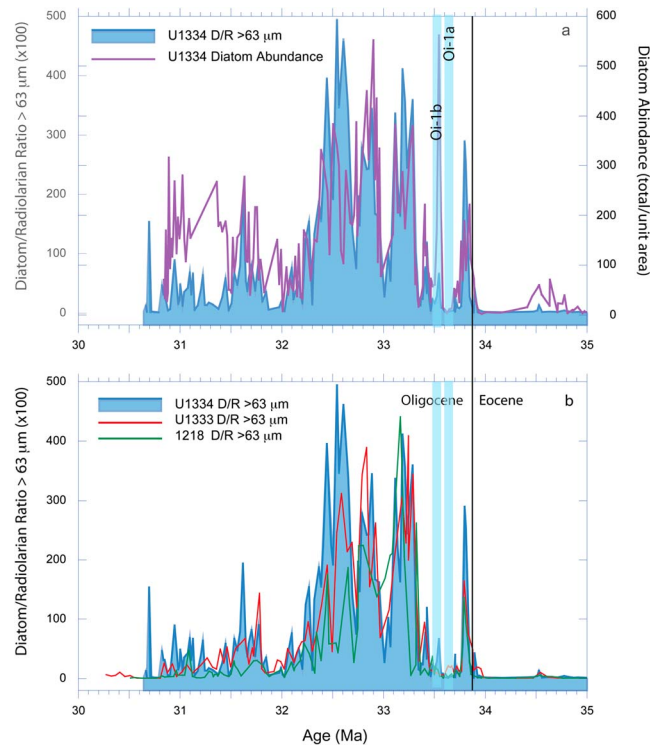


Figure 7. (a) Blue-filled curve, diatom to radiolarian ratio in the noncarbonate > 63 μm fraction of Site U1334. Purple curve, diatom abundance measured in 100 fields of view (cf. Figure 6c, see text) on strewn (settled) slide samples from Site U1334 [Baldauf, 2013]. (b) Blue-filled curve, diatom to radiolarian ratio in the noncarbonate > 63 μm fraction of Site U1334. Red curve and green curve, diatom to radiolarian ratio in the noncarbonate > 63 μm fraction of Sites U1333 and 1218, respectively. Data plotted versus age [Westerhold et al., 2014]. Light blue vertical bars and black line as in Figure 6.

There is no consistent offset in $\delta^{13}\text{C}$ between subbotinids and *Catapydrax unicavus* and *C. dissimilis* (Figure 4). Similar to $\delta^{18}\text{O}$, the interspecies $\delta^{13}\text{C}$ gradients vary over time. Offsets between shallow-living and deep-living planktonic forms are lowest in the basal Oligocene, including within the zone of abundant diatoms (32.3 Ma to 33.3 Ma; 224.5 rmcd to 234.8 rmcd), then increase as the abundance of diatoms declines (Figure 5, cf Figures 6 and 7).

3.2. Paleoproductivity

Mass accumulation rates for barite (BAR) [Erhardt et al., 2013] and opal [Lyle et al., 2005; Vanden Berg and Jarrard, 2004; Moore et al., 2008] show somewhat similar trends across the EOT with relatively high values in the uppermost Eocene that drop abruptly in the lowermost Oligocene (~33.7 Ma, ~239 rmcd) to fairly low values before recovering at ~33.55 Ma (~237 rmcd; Figures 6a and 6c). Opal accumulation rates in the lower Oligocene rise to values similar to those seen in the upper Eocene; however, BARs have generally lower minima and maxima in the Oligocene section compared to the upper Eocene [Erhardt et al., 2013] (Figure 6a). The overall average BAR in the Oligocene section is about half that

found in the upper Eocene. The BAR, even in the Eocene (~1 $\text{mg}/\text{cm}^2/\text{kyr}$), is distinctly lower than upper Pleistocene average BARs measured in the eastern tropical Pacific ($\geq 2 \text{ mg}/\text{cm}^2/\text{kyr}$ [Murray et al., 2012]).

In the modern equatorial Pacific we think of diatoms, an important part of the planktonic flora associated with nutrient-rich near-surface waters, as good indicators of high primary productivity [Smetacek, 1999]. The accumulation rate of their opaline frustules is thought to be the primary influence on opal accumulation rates in more modern deep-sea sediments [e.g., Murray et al., 1995]. However, diatoms are relatively scarce in the upper Eocene sediments (Figure 6c) and only become abundant in the lower Oligocene [Cervato and Burckle, 2003]. In the upper Eocene it is the radiolarians that deliver most of the opal to the seafloor [Moore et al., 2008]. Thus, the opal mass accumulation rate (MAR) data are similar to the diatom abundance in the Oligocene (correlation coefficient $r = 0.494$, Figure S1), but not in the Eocene. Taken together with the change in the average size of radiolarians across the EOT [Lazarus, 2009] these changes in the character of biogenic opal delivered to the sediment make it difficult to compare opal MAR as a proxy for export productivity in Eocene sediments to the same measure in Oligocene sediments. Opal MAR in the lower Oligocene is similar to that seen in the upper Pleistocene in the eastern tropical Pacific (average $< 0.07 \text{ g}/\text{cm}^2/\text{kyr}$; Murray et al. [2012]).

Within the Oligocene, diatom abundance reaches a broad maximum between 32.3 Ma and 33.3 Ma (~236–224 rmcd; Figures 6c and 7). This maximum is fairly closely matched by the interval of enhanced mixing suggested by the convergence of isotopic values of mixed-layer species *T. ampliapertura* and *D. venezuelana* (Figures 3 and 4) and by the relative abundance of large diatoms in the coarse fraction (>63 μm) of Site U1334 (Figure 7a). The prevalence of these large diatoms is similar to the pattern of total

diatom abundance (Figure 7a) and thus also relates to the export productivity of biogenic silica (Figure 6c). The pattern of large diatom abundance in Site U1334 is also similar to that seen in the other two sites studied (Figure 7b). Although differing in detail, the three sites each show three major D/R peaks in the lower Oligocene. Abundant large centric diatoms are uncommon in the tropical Pacific but have been noted in several, less well-sampled lower Oligocene sections in other tropical Pacific drill sites [e.g., Moore, 1973; Dinkelman, 1973; Nigrini *et al.*, 2006], with the dominant species in most samples being *Coscinodiscus excavatus*.

Estimates of primary productivity derived from BFAR [Herguera and Berger, 1991; Coxall and Wilson, 2011] are useful only in the Oligocene because of the strong dissolution of carbonate in the Eocene [Coxall and Wilson, 2011]. It should be noted, however, that the estimates of primary productivity shown here (Figure 6b) are at the low end of values used to calibrate the Herguera and Berger [1991] equation, particularly for the eastern equatorial Pacific where values of primary productivity just north of the equator reported by Loubere [2002] range from 90 to 160 gC/m²/yr, whereas primary productivity values estimated for the Oligocene range from 35 to 50 gC/m²/yr. The BFAR data on which these estimates are based are also markedly different, with the BFAR in Holocene to late glacial samples for the northeastern equatorial Pacific ranging from 135 to 207 specimens (>150 μm) per cm²/kyr [Herguera, 2000], whereas the Oligocene BFAR values range from near 0 to 46 per cm²/kyr, with an average of ~10 per cm²/kyr. To the extent that such comparisons can be made over such a large span of time, this would indicate that early Oligocene primary productivity in the eastern tropical Pacific was markedly lower than in more modern times.

At Oi-1a this primary productivity proxy is distinctly different from the opal MAR, BAR, and diatom abundance. However, post Oi-1a, the Oligocene primary productivity record (from BFAR), shows similar timing in maxima and minima to the BAR (e.g., blue dashed lines in Figure 6), although the amplitudes of their maxima and minima differ. This timing is also close to the maxima in eccentricity and minima in oxygen isotopes (Figure 6d).

The opal accumulation rate and diatom abundance data, in contrast, appear nearly antithetical to BAR and primary production estimates in the section above Oi-1a, with major peaks in diatom abundances nearly lining up with minima in BAR and primary productivity, as well as minima in eccentricity and maxima in oxygen isotopes (e.g., dashed red lines in Figure 6). This is even true in the upper Eocene where the relatively small peaks in diatom abundance line up with local minima in BAR.

The BFAR data set (Site 1218 [Coxall and Wilson, 2011]) is a very detailed record with sample spacing of 5 cm or less (red squares in Figure 6b). These data have been smoothed in Figure 6b to facilitate comparison with the other, less detailed records. If the diatom abundance data (Site U1334) is paired with primary productivity estimates that are taken from samples within 2 cm of the diatom samples (based on correlations between Site 1218 and Site U1334), a more detailed assessment can be made. As with the comparison of the plotted data, this pairing of data points is far from perfect in that not only are the measurements made on different samples but the samples are also from different sites that have been correlated at a scale of a decimeter [Westerhold *et al.*, 2012]. However, this pairing does show a very weak negative correlation ($r = -0.197$; Figure S2), similar to the apparent negative correlation between the plotted records (Figures 6b and 6c). A similar pairing of primary productivity data with BAR data (Site U1333, Figures 6a and 6b) gives only a slightly lower positive correlation ($r = 0.154$; Figure S3).

4. Discussion

4.1. Planktonic Foraminiferal Paleoecology

The isotopic paleoecologies of planktonic foraminifera can be used to gain insight into the dynamics of stratification in the upper water column. Here *Turborotalia ampliapertura* and *Dentoglobigerina venezuelana* consistently record the most negative $\delta^{18}\text{O}$ in comparison to the rest of the assemblage (Figures 2 and 3), indicative of calcification in the mixed layer [Wade *et al.*, 2007; Wade and Pearson, 2008; Wade *et al.*, 2012]. The stable isotope paleoecology of *D. venezuelana* has been controversial, with different studies indicating conflicting information on the depth of calcification [see Beltran *et al.*, 2014, and references therein]. Size-segregated stable isotope analysis indicates that specimens record a more positive $\delta^{18}\text{O}$ signal with increasing test size, suggesting sinking in the water column during gametogenesis. To attain enough specimens of *D. venezuelana*, our data are from a large size range (generally 250 μm and greater, Table S4); however, $\delta^{18}\text{O}$ values are consistently more negative than cooccurring subbotinids and *Catapsydrax*.

Subbotinids and paragloborotaliids have more positive $\delta^{18}\text{O}$ values in comparison to *Dentoglobigerina* and *Turborotalia* (Figures 2 and 3) supporting a thermocline dwelling habitat, consistent with previous studies [Poore and Matthews, 1984; Wade and Kroon, 2002; Wade et al., 2007]. *Catapsydrax* are well established as subthermocline dwellers [Poore and Matthews, 1984].

The interspecies planktonic $\delta^{13}\text{C}$ gradient is low, suggesting that none of these species had algal photosymbionts. Although chrysophyte symbionts might have been present, they would likely have little effect on the $\delta^{13}\text{C}$ [e.g., Bornemann and Norris, 2007, and references therein]. In addition, recrystallization could dampen the surface to deep $\delta^{13}\text{C}$ gradients measured in the planktonic foraminiferal tests [John et al., 2013].

4.2. Near-Surface Water Structure

The absence of a prominent and abundant diatom flora in the Eocene suggests that the Pacific equatorial divergence did not provide sufficient nutrients to the photic zone to allow such a flora to flourish. Yet there was a mound of biogenic sediments that persisted along the Pacific equator in the middle and upper Eocene (cf. Figure 1) [Moore et al., 2004]. These biogenic sediments were dominated by large, robust Eocene radiolarian tests with occasional carbonate accumulation events [Lyle et al., 2005; Pälike et al., 2012]. Such observations suggest weaker upwelling (or less nutrient-rich upwelled waters) and perhaps a relatively deep mixed layer with a broad nutricline. This would have provided a slightly higher productivity at the equatorial divergence, but with nutrient levels inadequate to support a dominant diatom flora. Modern radiolarians commonly have abundant photosymbionts, and from these symbionts radiolarians have the highest rates of primary production of all the sarcodine zooplankton [Caron et al., 1995]. The robust nature of the Eocene radiolarian tests [Lazarus et al., 2009; Moore, 1969] suggests that they migrated into the deeper waters where nutrients (including dissolved silica) were plentiful and returned to the photic zone where their symbionts could photosynthesize. This gave radiolarians a prominent role in productivity and the cycling of biogenic silica during the Eocene. Previous studies show that photosymbiotic species of planktonic foraminifera, calcareous analogues of some radiolaria, also decline from the late middle Eocene to Oligocene, suggesting that the changes in thermal and nutrient stratification were not limited to the eastern equatorial Pacific [Wade et al., 2008; Ezard et al., 2011].

During the late Eocene there were generally decreasing temperatures [Lear et al., 2008; Coxall and Wilson, 2011; Wade et al., 2012] and 47 radiolarian species and species groups became extinct in a series of three to four extinction events starting at the middle to late Eocene transition ~ 38 Ma [Kamikuri and Wade, 2012] and ending at the EOT itself [Moore and Kamikuri, 2012]. This preceded, and thus was not caused by, the onset of a dominant diatom flora in the early Oligocene.

Only a few radiolarian lineages continued across the E/O boundary. This suggests that the ecology of the equatorial divergence zone, as well as perhaps its vertical structure, nutrient richness, and source of the upwelled waters, may have started its dramatic change well before the EOT.

In the lower Oligocene the stable isotope data show a substantial increase in the gradients of oxygen and carbon isotopes between shallow and deeper calcifying species through the studied interval (Figures 3–5), starting with the lowest gradients in the basal Oligocene samples. If there has been no substantial diagenetic impact on the isotopic values, this pattern suggests a gradually increasing deep to shallow gradient in $\delta^{18}\text{O}$ values (i.e., temperature) and $\delta^{13}\text{C}$ values (i.e., nutrient availability), with the lowest gradients in the basal Oligocene. This is consistent with the Faul et al. [2000] study of the modern eastern equatorial Pacific where they found that the gradient in $\delta^{13}\text{C}$ between mixed-layer and thermocline planktonic foraminifera (their Tables 1 and 3) is lowest where the mixed layer is deep and highest where the mixed-layer depth is closer to the photic zone depth (thus closer to the top of the nutricline). This is similar to the results seen by Grant and Dickens [2002] for the late Miocene–early Pliocene in the western Pacific. An extremely low gradient in $\delta^{13}\text{C}$ was also found in the lowermost Oligocene and in the uppermost Eocene sections drilled in Tanzania [Wade and Pearson, 2008, Figure 4; John et al., 2013, Figure 5g]. This low gradient in the tropical Pacific together with very low estimates of export productivity (i.e., BAR, opal MAR, and diatom abundance) indicates a relatively deep mixed layer in the earliest Oligocene, with low-nutrient availability. This is in contrast to the results from the Tanzanian study of Dunkley Jones et al. [2008] who interpret the nannofossil assemblages across the EOT zone and into the lowermost Oligocene as indicating eutrophic conditions, as well as Ravizza and Paquay [2008] who suggest increased organic carbon burial in

latest Eocene and earliest Oligocene off Ghana in the tropical Atlantic. This difference may reflect the different environmental conditions at nearshore (Tanzania and offshore Ghana) versus open ocean locations but is not consistent with our interpretation of very low $\delta^{13}\text{C}$ gradients in the basal Oligocene found in this study and in Tanzania. This disconnect may indicate an increased nutrient supply from continental runoff during lowered sea level and, at least in the Tanzanian case, not from upward mixing of regenerated nutrients from the deeper waters.

The similarity between *Catapsydrax* and benthic foraminiferal oxygen isotope values suggests that there was little or no thermal gradient between the subthermocline and bottom waters in the Oligocene equatorial Pacific Ocean. We do not have comparable data from the Eocene because of poor carbonate preservation in the Eocene sections of these sites. However, other studies of Eocene sections in the tropical Pacific suggest that the deeper Eocene waters were relatively warm and rich in dissolved nutrients, including labile carbon [e.g., *Olivarez Lyle and Lyle*, 2006a, 2006b; *Pälike et al.*, 2009, 2012]. Depth gradients in $\delta^{13}\text{C}$ measured in the middle to upper Eocene of the tropical Indian Ocean (Tanzania [*John et al.*, 2013]) are on the order of 3‰.

Oxygen isotope data from the two mixed-layer species, *Turborotalia ampliapertura* and *Dentoglobigerina venezuelana*, vary in their isotopic values relative to each other, and their values converge in the middle range of the data shown here (Figures 3, ~32.2 and ~33.1 Ma). If this convergence is not a result of size variation in the specimens measured (Table S4), this limited sequence of data suggests there may have been enhanced mixing of the near-surface ocean during this interval. It is within this middle range of the lower Oligocene that two samples contain subbotinid species that may represent thermocline dwellers: one containing *Subbotina eoacena* and one, *S. corpulenta* (Figures 3 and 4). Both show $\delta^{18}\text{O}$ values somewhat more positive than those above and below this level by other subbotinids (Figure 3). If *S. eoacena* in particular can be taken as a thermocline dweller, its more positive values in this interval suggest a colder thermocline.

The first strong peak in diatom abundance and opal accumulation rates occurred during Oi-1b (33.55 Ma, ~237 rmcd; Figure 6c) and appears to be the first move toward a more “modern” vertical structure in the eastern equatorial Pacific, with a nutrient-rich upwelling zone and abundant diatoms. This did not occur until more than 100 kyr after the EOT itself. With the first strong showing of diatoms, the character of the diatom assemblage included an unusual abundance of large centric diatoms (Figure 7). A similar blossoming of large centric diatoms is not encountered again in this region until near the Oligocene-Miocene boundary [*Pälike et al.*, 2009]. In general, smaller diatoms have an ecologic advantage because of their rapid uptake of nutrients and fast growth and reproduction rates. Large diatoms have a competitive advantage only in cases when it is important to be able to store nutrients or to migrate to deeper depths where nutrients are more readily available [*Litchman et al.*, 2009]. In the data presented here, the similarity of the total diatom abundance and the relative abundance of large diatoms (Figure 7a) may indicate a pulsed (perhaps seasonal) supply of nutrients in which the smaller diatoms would have the advantage directly after such a pulse, whereas the larger diatoms might have the advantage later in the period when nutrient storage and/or migration becomes important [*Litchman et al.*, 2009]. However, the resolution of our records does not require such a seasonal scenario. It is also possible that interannual, decadal, or even longer-term variability in upwelling would periodically favor the larger diatoms.

This assemblage of large and small diatoms suggests either a periodically deep nutricline or a strongly pulsed nutrient supply from equatorial divergence or advection from coastal upwelling off South America (or both). The gradual increase in the deep to shallow isotopic gradients suggests a gradual change in the vertical structure and stability of the upper water column that was favorable for a mix of large and small diatoms (Figure 7a) for about 1 Myr, followed by a more usual size distribution of the diatom flora (i.e., dominated by the smaller forms). Isotopic gradients in the youngest part of the Oligocene record are comparable to those found at a similar location in the modern equatorial Pacific (e.g., RC13-113) [*Faul et al.*, 2000].

Only seven D/R data points lie within 10 cm (range of 1 cm to 8 cm) of data for the $\delta^{13}\text{C}$ gradients between subthermocline and mixed-layer planktonic foraminifera shown here (Figure 5); however, the pairing of these data shows a slight tendency of higher D/R values (i.e., more large diatoms) when the $\delta^{13}\text{C}$ gradient is lower (i.e., the mixed layer is deeper) (Figure 8a). When the seven D/R data points are compared to the difference in isotopic values of *Turborotalia ampliapertura* and *Dentoglobigerina venezuelana* (mixed-layer

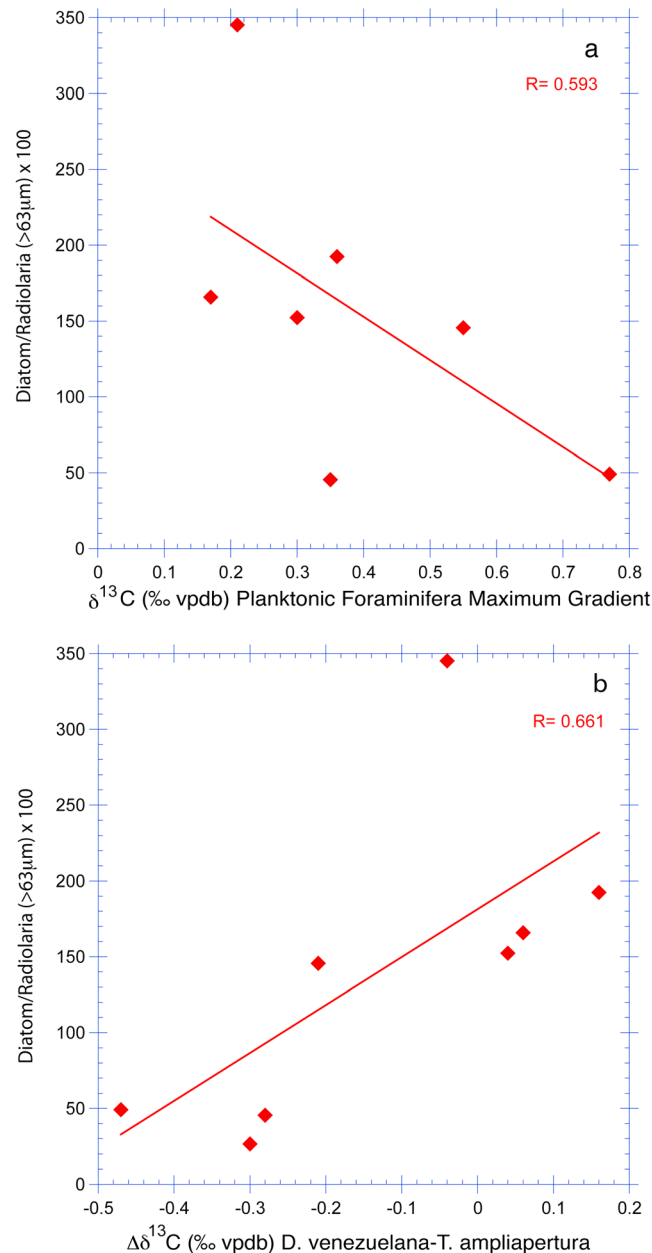


Figure 8. Diatom to radiolarian abundance ratio compared to (a) maximum gradient in $\delta^{13}\text{C}$ of planktonic foraminifera (cf. Figure 5) and (b) difference in the $\delta^{13}\text{C}$ values of *Turborotalia ampliapertura* and *Dentoglobigerina venezuelana* (cf. Figure 4). Data are from paired samples taken within 1 to 8 cm of each other (see text).

species), there is no significant relationship between D/R values and the difference in $\delta^{18}\text{O}$ values; however, there is a reasonably strong correlation between D/R values and the difference in $\delta^{13}\text{C}$ values of the two species (Figure 8b). When the $\delta^{13}\text{C}$ of *T. ampliapertura* is larger than that of *D. venezuelana*, D/R values are lower; when *T. ampliapertura* $\delta^{13}\text{C}$ values are lower than those of *D. venezuelana*, D/R values tend to be larger. Wade *et al.* [2012] suggested that *T. ampliapertura* calcified at deeper depths or had a cooler season of growth in the Oligocene of the Gulf of Mexico. If this observation applies to the eastern equatorial Pacific, where the cooler season is associated with equatorial upwelling, then increased values of $\delta^{13}\text{C}$ in *T. ampliapertura* may signify times of upwelling when larger diatoms would not have a strong advantage over the smaller forms, whereas increased values of $\delta^{13}\text{C}$ in *D. venezuelana* would indicate times of a relatively deep mixed layer and weaker upwelling. Taken together with the apparent relationship between D/R numbers and the overall $\delta^{13}\text{C}$ gradient in the upper waters of the eastern equatorial Pacific (Figure 8a), this seems to suggest that *D. venezuelana* may have lived higher up in the mixed layer where $\delta^{13}\text{C}$ is higher and that the bigger diatoms formed a larger part of the diatom flora when the mixed layer is relatively deep. This is consistent with the observations of Litchman *et al.* [2009] concerning size dependence of diatom ecology and with the higher values of $\delta^{18}\text{O}$ in subbotinids found in the interval of abundant large diatoms (~32.3 Ma–33.3 Ma).

4.3. Paleoproductivity

4.3.1. General Patterns of Paleoproductivity Change

Globally, the transition between the late Eocene and early Oligocene had a profound impact on the productivity, planktonic community structure, and ecology of the oceans [e.g., Diester-Haass, 1995; Diester-Haass and Zahn, 1996; Salamy and Zachos, 1999; Anderson and Delaney, 2005; Scher and Martin, 2006; Dunkley Jones *et al.*, 2008; Pearson *et al.*, 2008; Erhardt *et al.*, 2013]. The general picture given by several studies is that oceanic productivity in high southern latitudes was high in the late Eocene, continuing into the early Oligocene [e.g., Diester-Haass and Zahn, 1996; Salamy and Zachos, 1999; Latimer and Filippelli, 2002;

Anderson and Delaney, 2005; Egan et al., 2013]; however, these studies may have missed intervals near the E/O boundary itself because of hiatuses and incomplete section recovery. In the tropical ocean, export production dropped in the lower Oligocene [Nilsen et al., 2003; Schumacher and Lazarus, 2004; Erhardt et al., 2013].

The data sets presented here agree with this pattern for the eastern equatorial Pacific; there is generally higher export productivity in the late Eocene, dropping to lower values after Oi-1. Looking at the broad general patterns of early Oligocene paleoproductivity given by the proxies used here, we see that BAR did not fully recover from the sharp drop at the EOT until after ~33.2 Ma (Figure 6a). Diatoms began an interval of higher abundance near 33.3 Ma. The maxima in diatom abundance (particularly large diatoms) ended near 32.3 Ma (Figures 6c and 7). Primary productivity estimates (based on BFAR) had, on average, higher values after 32.3 Ma (Figure 6a) coincident with a slight increase in benthic foraminiferal oxygen isotope values (Figure 6d) and close in timing to the addition of “northern component waters” to the deep waters of the Southern Ocean [Via and Thomas, 2006]. Thus, we see a sequence of changes in the average response of these paleoproductivity proxies that mirrors the increasing isotopic gradients on the planktonic foraminifera (Figure 5) and the shoaling of the thermocline. There is a suggestion of increasing productivity that accompanies the shoaling thermocline from the estimates of primary productivity (from BFAR) and a shift in ecology to the more usual size distribution of diatoms. This may have resulted from a slight increase in nutrient content of the southern mode waters [Sarmiento et al., 2004] that fed the upwelling in the eastern tropical Pacific once northern source waters reached the deep waters of the Southern Ocean. The BAR, on average, is only slightly higher after 32.3 Ma than between 33.3 Ma and 32.3 Ma (Figure 6a).

4.3.2. Proxies of Paleoproductivity

When comparing the detailed Oligocene records of the four paleoproductivity proxies presented here (Figure 6), there are two glaring inconsistencies: (1) the peak in primary productivity (BFAR) at Oi-1a where all other proxies indicate very low export productivity and (2) the nearly antithetical relationship of diatom abundance and opal accumulation rates with BAR and primary productivity.

The peak in estimated primary productivity at Oi-1a led Coxall and Wilson [2011] to propose higher productivity in this interval with a connection to high-latitude conditions. As shown here, all other paleoproductivity proxies show minima at Oi-1a. There are a couple of possible explanations for this. First, the precipitous drop in the calcite compensation depth at the end of the Eocene led to a rapid accumulation of calcareous microfossils in basal Oligocene sediments. This great increase in the rain and accumulation of biogenic material at the sea floor, together with any scavenged dissolved organic carbon carried by the particles, may have given a boost to the benthic population [cf. Francois et al., 2002; Henson et al., 2012] or at least the fossilization potential of their accumulating tests. A second (and perhaps more likely) explanation is associated with the physical and chemical characters of the bottom waters themselves in the earliest Oligocene. They were markedly colder than in the late Eocene [Liu et al., 2009] and therefore could carry more dissolved oxygen, an environmental variable believed to be important to the benthic assemblage [Loubere, 1994; Fariduddin and Loubere, 1997; Van der Zwaan et al., 1999]. In addition, the turbulence of the bottom waters at this site in the earliest Oligocene appears to have been enhanced [Moore, 2013], and this is also an environmental variable that, in moderation, appears to be beneficial to the benthic community [Levin and Thomas, 1989; Gooday, 1994; Aller, 1997; Hayward et al., 2002]. The earliest peak in primary productivity lies between the final two maxima in the reworking of older radiolarians measured at the same site (Site 1218) [Moore, 2013] and near the maximum in reworked older nannofossils found in the Tanzania cores [Dunkley Jones et al., 2008]. Erhardt et al. [2013] have suggested that the reworked uppermost Eocene sediments may have provided an additional food source for the benthic community in the basal Oligocene.

The approximately antithetical nature of diatom abundance with BAR throughout the record and with primary productivity estimates through most of the Oligocene is a bit more difficult to explain. In the upper Pleistocene of the eastern tropical Pacific, variation in opal MAR (and presumably diatom abundance) is positively correlated with BAR ($r = 0.69$ [Murray et al., 2012]). Whereas in the Eocene-Oligocene records of BAR [Erhardt et al., 2013] tend to be coherent and in phase with high carbonate (particularly at the longer periods that could be resolved in their data), and in the Eocene at least, in phase with warmer temperatures. We associate diatom abundance with upwelling, cooler temperatures, and lower carbonate concentrations in pelagic sediments. Thus, the lack of agreement between diatom abundance and BAR seen

here may, in part, result from a difference in the phase of the response of diatoms versus carbonate producers to cyclic oceanographic change.

The benthic foraminiferal assemblage in Site 1218 [Takata *et al.*, 2010] does not support the scenario of strong seasonality in the benthic food supply. The assemblage factor dominated by *Epistominella exigua*, a benthic species associated with a pronounced seasonal supply of phytodetritus, accounts for less than 3% of the variance in the Oligocene fauna [Takata *et al.*, 2010, and references therein]. Thomas and Gooday [1996] in their survey of deep-sea benthic foraminifera across the E/O boundary see a decrease in species diversity and an increase in phytodetritus-exploiting species in high latitudes, which they attribute to an increased, but highly seasonal, food influx. In contrast, at low latitudes species diversity increased across the E/O boundary, without a strong indication of seasonality in food supply.

The apparently very low paleoproductivity in the eastern equatorial Pacific of the Oligocene may not have been enough to support benthic species that thrive on seasonal supply of detritus even though seasonal variation in nutrient richness did affect the diatom assemblage. This disconnect between the BFAR-based primary productivity estimates and the variation in diatom abundance may also result from other factors that affect export productivity. Laws *et al.* [2000] in their modeling study of export production relative to temperature and net primary productivity found that at moderate to high productivity rates (as might be expected seasonally in the eastern equatorial Pacific) export productivity is not very sensitive to total production and is negatively correlated with temperature. This model assumes that the food web adjusts to maintain a degree of stability that requires “new production” be equal to “export production.” The amount of variation in our records indicates that this assumed degree of stability does not hold over the long term. Nevertheless, this model may indicate that the pulses of productivity evidenced by the variation in diatom abundance were not readily exported to the benthos under the conditions of the early Oligocene. In addition, Henson *et al.* [2012] indicate that the particle export efficiency in tropical latitudes is low and that there is a negative correlation between the fraction of organic matter that reaches the deep ocean and opal export flux, but no correlation with carbonate export flux.

The approximate alignment of high eccentricity with high BAR and primary productivity and low eccentricity with high diatom abundance and opal MAR further complicates comparison to more modern times. Although the resolution of the data presented here does not allow a full comparison with Milankovitch orbital variations, it is apparent that such variations are associated with variations in deep-sea sediments of the Oligocene and Eocene [e.g., Pälike *et al.*, 2006; Westerhold *et al.*, 2014] as well as the sediments of the Pleistocene. Thus, it is not surprising that there is a degree of similarity between variations seen in the paleoproductivity proxies and the longer period, eccentricity record (Figure 6). What is surprising is the antithetical nature of this relationship, with BAR and primary productivity (BFAR) estimates associated with high eccentricity and diatom abundance and opal MAR with low eccentricity.

Taking the simplest view that low eccentricity is associated with cool summers and warm winters, it would seem that opal MAR and diatom abundance may be related to relatively low levels of equatorial divergence (i.e., low overall productivity). Whereas high eccentricity, associated with warm summers and cold winters, might result in stronger seasonal advection of nutrient-rich upwelled waters from the South American coast [e.g., Herguera, 2000] (Figure 1). This apparently simple relationship is not seen in the upper Pleistocene [e.g., Weber and Pisias, 1999; Murray *et al.*, 2012].

There is another observation that relates the chemical character of the deep water to BAR. Productivity in the high southern latitudes increased markedly in the late Eocene. Salmay and Zachos [1999] using opal accumulation rates in Site 744 and Diester-Haass [Diester-Haass, 1995; Diester-Haass and Zahn, 1996] using the accumulation rates of radiolarians and diatoms in Sites 689B and 690 showed variation in these paleoproductivity proxies through the upper Eocene into the lower Oligocene. Recovery of the sections at these sites was not complete; thus, it is difficult to confidently correlate these high-latitude sites to those studied here. But it is possible that variation in the recycled nutrient richness of waters sourced in high latitudes affected the degree of barite saturation in the low-latitude deep and intermediate waters. This may have had an impact on the rate of formation of barite in tropical latitudes [Paytan and Griffith, 2007] that to some degree obscured the relationship of BAR to local productivity.

4.4. Opening of Ocean Gateways

The opening of high-latitude oceanic gateways during the late Eocene and early Oligocene have often been seen as contributing to, if not causing, the cooling of southern high-latitude surface and deep waters

[e.g., Kennett and Shackleton, 1976; Liu et al., 2009], and the associated pulses of higher paleoproductivity in high southern latitudes [e.g., Diester-Haass, 1995; Salamy and Zachos, 1999]. Because the upwelled waters in the tropics were likely derived from the high southern latitudes carrying regenerated nutrients [e.g., Sarmiento et al., 2004], the timing and extent of these openings are important considerations in understanding paleoproductivity changes in the tropical Pacific. The opening of the Tasman Passage is reasonably well constrained to the latest Eocene–earliest Oligocene [Stickley et al., 2004]. The opening of the Drake Passage, however, is still a matter of much debate [Barker et al., 2007]. The geometry of the opening of the Drake Passage is considerably more complicated than the Tasman Passage, and it is very likely that the opening itself was a complex process [e.g., Livermore et al., 2007; Dalziel et al., 2013]. Evidence for the earliest opening in the middle Eocene comes from neodymium isotopes [e.g., Scher and Martin, 2004, 2006]. Evidence for an opening near the E/O boundary comes from tectonic reconstructions and sedimentological studies [Barker and Burrell, 1977; Lawver and Gahagan, 1998, 2003; Latimer and Filippelli, 2002; Livermore et al., 2005, 2007; Pfuhl and McCave, 2005]. Two studies, one based on nearby sedimentological data [Latimer and Filippelli, 2002] and one on plate reconstructions [Lawver and Gahagan, 2003], suggest at least a substantial shallow opening by ~32 Ma–32.8 Ma. A full opening and a full development of the Antarctic Circumpolar Current in the late Oligocene–early Miocene is evidenced by strong sediment erosion at high latitudes in the Southern Ocean [e.g., Kennett and Barker, 1990; Lyle et al., 2008; Dalziel et al., 2013] and increased offsets in deep water $\delta^{13}\text{C}$ gradients [Katz et al., 2011].

Many coupled general circulation model studies have explored the impact of these gateway openings. These studies have come to two important conclusions: (1) changes in atmospheric CO_2 likely controlled the dramatic cooling and ice sheet buildup at the EOT [Huber and Sloan, 2001; Huber et al., 2004; Huber and Nof, 2006; Sijp et al., 2009, 2011; Liu et al., 2009] and (2) the impact of the gateway openings themselves had an effect on the circulation patterns and sea surface temperatures at high latitudes, as well as deep water temperatures, vertical ocean structure, and meridional overturning [Nong et al., 2000; Liu et al., 2009; Sijp and England, 2004; Sijp et al., 2009, 2011; Zhang et al., 2010, 2011; Yang et al., 2013]. However, it is difficult for these models to explore in detail the complexities of a long-term opening and deepening of these two key passages when their detailed history and phasing is inadequately understood [Hill et al., 2013].

It is generally agreed that the opening of the southern gateways led to large-scale cooling of shallow and deep waters in the high southern latitudes [Nong et al., 2000; Sijp and England, 2004; Sijp et al., 2009, 2011; Liu et al., 2009; Zhang et al., 2010, 2011; Yang et al., 2013]. The sensitivity of sea surface temperature in high latitudes to changes in atmospheric CO_2 and the vigor of Antarctic Bottom Water formation is greater when the Drake Passage is closed than when it is open [Sijp et al., 2009; Sijp and England, 2004]. The deepening of the Tasman Passage to >1300 m would lead to a cooling of deep waters in the Pacific [Sijp et al., 2011; Liu et al., 2009] and to a warming and deepening of the thermocline in middle and low latitudes [Toggweiler and Bjornsson, 2000; Sijp and England, 2004; Sijp et al., 2011], as well as more than a doubling in tropical precipitation over evaporation [Sijp et al., 2011]. This deeper thermocline combined with increased rainfall in the tropics would have tended to suppress upwelling and equatorial productivity, which is consistent both with what we see during the Oi-1a interval in our export productivity proxies (Figure 6) and in the isotopic gradients in the basal Oligocene (Figures 3–5). The transient nature of this relatively brief period of low export productivity suggests that the timing and magnitude of the Drake Passage opening may have had a critical impact on near-surface waters north of the Antarctic Circumpolar Current [Sijp et al., 2009, 2011].

5. Conclusions

Most of the paleoproductivity proxies presented here sharply decreased at Oi-1 from the relatively high values in the Eocene to very low values in the basal Oligocene sediments of the eastern equatorial Pacific. Combining the information on paleoproductivity, model reconstructions, and stable isotope measurements of planktonic foraminifera, we see a transition from a warm to a cold climate that caused a sharp reduction in equatorial export productivity immediately following the EOT. We believe this reduction in paleoproductivity estimates was caused by a deepening of the thermocline and an overall increase in the stability of the upper ocean of the tropics. After a few hundred thousand years (and perhaps accompanying changes in the high-latitude gateways) the thermocline appears to have shoaled, allowing the large diatoms to access nutrients by depth migration. The transient nature of this relatively brief period of

low paleoproductivity suggests that the timing and magnitude of the Drake and Tasman Passage openings may have been critical to their impact on the region north of the Antarctic Circumpolar Current [Sijp *et al.*, 2009, 2011].

With some degree of seasonal upwelling, paleoproductivity began to increase. A continued shoaling of the thermocline (perhaps in association with a deepening of the Drake Passage near 32.3 Ma [Latimer and Filippelli, 2002] and the inception of northern component water feeding into the Southern Ocean [Via and Thomas, 2006; Sijp *et al.*, 2009]) gave the ecologic advantage to smaller diatoms during pulses of nutrient supply and is associated with higher average estimates of primary productivity (based on BFAR). However, paleoproductivity in the early Oligocene appears to have been lower than in the late Eocene and never reached the even higher values found in the eastern equatorial Pacific in more modern times.

The fact that the BAR and BFAR productivity proxies are nearly antithetical to diatom abundance seems to suggest that the total annual food supply to the deep-sea benthic community was actually diminished during intervals with pulses of high nutrients in the photic zone evidenced by diatom abundance and opal accumulation rates. This is consistent with the findings of Henson *et al.* [2012] that show a negative correlation of opal flux and the fraction of organic carbon that reaches the deep-sea floor. In our data the relation of BAR, in particular, with opal MAR and diatom abundance is apparently opposite to that seen in the upper Pleistocene. Furthermore, the average opal MAR is the only paleoproductivity proxy that shows little or no difference between upper Pleistocene and lower Oligocene times—except in the phase of its relationship to these other variables.

We are not claiming that eccentricity drives the productivity in the tropical Pacific during the Eocene–Oligocene interval shown here; however, through its modulation of precession and interaction with tilt, it does have a role to play. Unfortunately, sample resolution in this study only allows us to make useful comparisons with this longer-period orbital variable and does not allow us to examine the detailed differences in phasing between primary productivity, diatom abundance, opal MAR, and BAR relative to any other Milankovitch forcings of climate and productivity change.

Our comparison of different paleoproductivity proxies gives a fairly consistent picture of long-term changes in productivity across the EOT and into the Oligocene, but in detail, our records emphasize the fact that although each of these proxies may be “a measure” of paleoproductivity, all of them are affected by other factors such as upper water structure, the chemical and physical nature of the deep waters, as well as differences between what is produced in the photic zone, is exported to deeper waters and is eventually deposited on the sea floor. Thus, none of these proxies is “the measure” of paleoproductivity and should be evaluated with full knowledge of those other factors that affect the records. In their imperfections lie clues to other environmental conditions.

Acknowledgments

The authors wish to thank H. Pälke (University of Bremen) and H. Nishi (Tohoku University) for their leadership and guidance during and after IODP Expedition 320. Joanne Reuss provided invaluable lab assistance in preparing samples used in this study. Samples were provided by the Integrated Ocean Drilling Program (IODP), which is sponsored by the U.S. National Science Foundation and participating countries. The work of T.M. was financially supported by a contract with the Consortium for Ocean Leadership. Planktonic foraminiferal sample preparation and stable isotope analyses were funded by a NSF CAREER award (EAR-0847300) and a Natural Environment Research Council grant (NE/G014817/1) to B.W. T.W. received support from the Deutsche Forschungsgemeinschaft (DFG).

References

- Aller, J. Y. (1997), Benthic community response to temporal and spatial gradients in physical disturbance within a deep-sea western boundary region, *Deep Sea Res., Part I*, 44(1), 39–69.
- Anderson, L. D., and M. L. Delaney (2005), Middle Eocene to early Oligocene paleoceanography from Agulhas Ridge, Southern Ocean (Ocean Drilling Program Leg 177, Site 1090), *Paleoceanography*, 20, PA1013, doi:10.1029/2004PA001043.
- Baldauf, J. G. (2013), Data report: Diatoms from Sites U1334 and U1338, Expedition 320/321, in *Proc IODP*, vol. 320/321, edited by H. Pälke *et al.*, pp. 1–8, Integr. Ocean Drill. Program, College Station, Tex., doi:10.2204/ioldp.proc.320321.215.2013.
- Barker, P. F., and J. Burrell (1977), The opening of Drake Passage, *Mar. Geol.*, 25, 15–34.
- Barker, P. F., G. M. Filippelli, F. Florindo, E. E. Martin, and H. D. Scher (2007), Onset and role of the Antarctic Circumpolar Current, *Deep Sea Res., Part II*, 54, 2388–2398.
- Beltran, C., G. Rousselle, J. Backman, B. S. Wade, and M. A. Sicre (2014), Paleoenvironmental conditions for the development of calcareous nannofossil acme during the late Miocene in the Eastern Equatorial Pacific, *Paleoceanography*, 29, 210–222, doi:10.1002/2013PA002506.
- Bohaty, S. M., and J. C. Zachos (2003), Significant Southern Ocean warming event in the late middle Eocene, *Geology*, 31, 1017–1020.
- Bornemann, A., and R. D. Norris (2007), Size-related stable isotope changes in Late Cretaceous planktic foraminifera: Implications for paleoecology and photosymbiosis, *Mar. Micropaleontol.*, 65, 32–42, doi:10.1016/j.marmicro.2007.05.005.
- Caron, D. A., A. F. Michaels, N. R. Swanberg, and F. A. Howse (1995), Primary productivity by symbiont-bearing planktonic sarcodines (Acantharia, Radiolaria, Foraminifera) in surface waters near Bermuda, *J. Plank. Res.*, 17(1), 103–129.
- Cervato, C., and L. H. Burckle (2003), Pattern of first and last appearance in diatoms: Oceanic circulation and the position of the Polar Fronts during the Cenozoic, *Paleoceanography*, 18(2), 1055, doi:10.1029/2002PA000805.
- Coxall, H. K., and P. A. Wilson (2011), Early Oligocene glaciation and productivity in the eastern equatorial Pacific: Insights into global carbon cycling, *Paleoceanography*, 26, PA2221, doi:10.1029/2010PA002021.

- Coxall, H. K., P. A. Wilson, H. Pälike, C. H. Lear, and J. Backman (2005), Rapid stepwise onset of Antarctic glaciation and deeper calcite compensation in the Pacific Ocean, *Nature*, *433*(7021), 53–57, doi:10.1038/nature03135.
- Dalziel, I. W. D., L. A. Lawver, J. A. Pearce, P. F. Barker, A. R. Hastie, D. N. Barford, H.-W. Schenke, and M. B. Davis (2013), A potential barrier to deep Antarctic circumpolar flow until the late Miocene?, *Geology*, *41*(9), 947–950, doi:10.1130/G34352.1.
- DeConto, R. M., and D. Pollard (2003), Rapid Cenozoic glaciation of Antarctica triggered by declining atmospheric CO₂, *Nature*, *421*, 245–249.
- Diester-Haass, L. (1995), Middle Eocene to early Oligocene paleoceanography of the Antarctic Ocean (Maud Rise, ODP 13, Site 689): Change from a low to a high productivity ocean, *Palaeogeogr. Palaeoclimatol. Palaeoecol.*, *113*, 311–334.
- Diester-Haass, L., and R. Zahn (1996), Eocene-Oligocene transition in the Southern Ocean: History of water mass circulation and biological productivity, *Geology*, *24*, 163–166, doi:10.1130/0091-7613.
- Dinkelman, M. G. (1973), Radiolarian stratigraphy: Leg 16, Deep Sea Drilling Project, in *Initial Report DSDP*, vol. 16, edited by T. J. van Andel et al., pp. 747–813, U.S. Government Printing Office, Wash., doi:10.2973/dsdp.proc.16.128.1973.
- Dunkley Jones, T., P. R. Bown, P. N. Pearson, B. Wade, H. Coxall, and C. H. Lear (2008), Major shifts in calcareous phytoplankton assemblages through the Eocene-Oligocene transition of Tanzania and their implications for low-latitude primary production, *Paleoceanography*, *23*, A4204, doi:10.1029/2008PA001640.
- Dymond, J., E. Suess, and M. Lyle (1992), Barium in deep-sea sediment: A geochemical proxy for paleoproductivity, *Paleoceanography*, *7*, 163–181, doi:10.1029/92PA00181.
- Eagle, M., A. Paytan, K. R. Arrigo, G. van Dijken, and R. W. Murray (2003), A comparison between excess barium and barite as indicators of carbon export, *Paleoceanography*, *18*(1), 1021, doi:10.1029/2002PA000793.
- Egan, K. E., R. E. M. Rickaby, K. R. Hendry, and A. N. Halliday (2013), Opening the gateways for diatoms primes Earth for Antarctic glaciation, *EPSL*, *375*, 34–43.
- EGGE, J. K., and D. L. Aksnes (1992), Silicate as a regulating nutrient in phytoplankton competition, *Mar. Ecol. Prog. Ser.*, *83*, 281–289.
- Erhardt, A. M., H. Pälike, and A. Paytan (2013), High-resolution record of export production in the eastern equatorial Pacific across the Eocene-Oligocene transition and relationships to global climatic records, *Paleoceanography*, *28*, 1–13, doi:10.1029/2012PA002347.
- Exon, N. F., J. P. Kennett, and M. J. Malone (2004), Leg 189 synthesis: Cretaceous–Holocene history of the Tasmanian Gateway, in *Proceedings ODP, Science Results*, vol. 189, edited by N. F. Exon et al., pp. 1–37, Ocean Drill. Program, College Station, Tex., doi:10.2973/odp.proc.sr.189.101.2004.
- Ezard, T. H. G., T. Aze, P. N. Pearson, and A. Purvis (2011), Interplay between changing climate and species' ecology drives macroevolutionary dynamics, *Science*, *332*, 349–351.
- Fariduddin, M., and P. Loubere (1997), The surface ocean productivity response of deeper water benthic foraminifera in the Atlantic Ocean, *Mar. Micropaleontol.*, *32*, 289–310.
- Faul, K. L., and M. L. Delaney (2010), A comparison of early Paleogene export productivity and organic carbon burial flux for Maud Rise, Weddell Sea, and Kerguelen Plateau, south Indian Ocean, *Paleoceanography*, *25*, PA3214, doi:10.1029/2009PA001916.
- Faul, K. L., A. C. Ravelo, and M. L. Delaney (2000), Reconstructions of upwelling, productivity, and photic zone depth in the eastern equatorial Pacific ocean using planktonic foraminiferal stable isotopes and abundances, *J. Foram. Res.*, *30*(2), 110–125.
- Feely, R. A., M. Lewison, G. L. Massoth, G. Robert-Baldo, J. W. Lavelle, R. H. Byrne, K. L. Von-Damm, and H. C. Curl (1987), Composition and dissolution of black smoker particulates from active vents on the Juan de Fuca Ridge, *J. Geophys. Res.*, *92*, 11,347–11,363, doi:10.1029/JB092iB11p11347.
- Feely, R. A., T. L. Geiselman, E. T. Backer, G. J. Massoth, and S. R. Hammond (1990), Distribution and composition of hydrothermal plume particles from the ASHES vent field at Axial volcano, Juan de Fuca Ridge, *J. Geophys. Res.*, *95*, 12,855–12,873, doi:10.1029/JB095iB08p12855.
- Francois, R., S. Honjo, R. Krishfield, and S. Manganini (2002), Factors controlling the flux of organic carbon to the bathypelagic zone of the ocean, *Global Biogeochem. Cycles*, *16*(4), 1087, doi:10.1029/2001GB001722.
- Funakawa, S., H. Nishi, T. C. Moore, and C. A. Nigrini (2006), Radiolarian faunal turnover and paleoceanographic change around Eocene/Oligocene boundary in the central equatorial Pacific, ODP Leg 199, Holes 1218A, 1219A, and 1220A, *Palaeogeogr. Palaeoclimatol. Palaeoecol.*, *230*, 183–203, doi:10.1016/j.palaeo.2005.07.014.
- Gooday, A. J. (1994), The biology of deep-sea foraminifera: A review of some advances and their significance in paleoecology, *Palaios*, *9*, 14–31.
- Gooday, A. J., and A. E. Rathburn (1999), Temporal variability in living deep-sea benthic foraminifera: A review, *Earth Sci. Rev.*, *4*, 187–212.
- Grant, K. M., and G. R. Dickens (2002), Coupled productivity and carbon isotope records in the southwest Pacific Ocean during the late Miocene–early Pliocene biogenic bloom, *Palaeogeogr. Palaeoclimatol. Palaeoecol.*, *187*, 61–82.
- Griffith, E., M. Calhoun, E. Thomas, K. Averyt, A. Erhardt, T. Bralower, M. Lyle, A. Olivarez Lyle, and A. Paytan (2010), Export productivity and carbonate accumulation in the Pacific Basin at the transition from a greenhouse to icehouse climate (late Eocene to early Oligocene), *Paleoceanography*, *25*, PA3212, doi:10.1029/2010PA001932.
- Hayward, B. W., H. Neil, R. Carter, H. R. Grenfell, and J. J. Hayward (2002), Factors influencing the distribution patterns of Recent deep-sea benthic foraminifera, east of New Zealand, Southwest Pacific Ocean, *Mar. Micropaleontol.*, *46*, 139–176.
- Henson, S. A., R. Sanders, and E. Madsen (2012), Global patterns in efficiency of particulate organic carbon export, and transfer to the deep ocean, *Global Biogeochem. Cycles*, *26*, GB1028, doi:10.1029/2011GB004099.
- Herguera, J. C. (2000), Last glacial paleoproductivity patterns in the eastern equatorial Pacific: Benthic foraminifera records, *Mar. Micropaleontol.*, *40*, 259–275.
- Herguera, J. C., and W. H. Berger (1991), Paleoproductivity from benthic foraminifera abundance: Glacial to postglacial change in the west-equatorial Pacific, *Geology*, *19*, 1173–1176.
- Hill, D. J., A. M. Haywood, P. J. Valdes, J. E. Francis, D. J. Lunt, B. S. Wade, and V. C. Bowman (2013), Paleogeographic controls on the onset of the Antarctic Circumpolar Current, *Geophys. Res. Lett.*, *40*, 5199–5204, doi:10.1002/grl.50941.
- Huber, M., and D. Nof (2006), The ocean circulation in the southern hemisphere and its climatic impacts in the Eocene, *Palaeogeogr. Palaeoclimatol. Palaeoecol.*, *231*, 9–28.
- Huber, M., and L. C. Sloan (2001), Heat transport, deep waters and thermal gradients: Coupled simulation of an Eocene “greenhouse” climate, *Geophys. Res. Lett.*, *28*, 3481–3484, doi:10.1029/2001GL012943.
- Huber, M., H. Brinkhuis, C. E. Stickley, K. Doos, A. Sluijs, J. Warnaar, S. A. Schellenberg, and G. L. Williams (2004), Eocene circulation of the Southern Ocean: Was Antarctica kept warm by subtropical waters?, *Paleoceanography*, *19*, PA4026, doi:10.1029/2004PA001014.
- John, E., P. N. Pearson, H. B. Birch, H. K. Coxall, B. S. Wade, and G. L. Foster (2013), Warm ocean processes and carbon cycling in the Eocene, *Phil. Trans. R. Soc. A*, *371*, doi:10.1098/rsta.2013.0099.

- Kamikuri, S., and B. S. Wade (2012), Radiolarian magnetobiochronology and faunal turnover across the middle/late Eocene boundary at Ocean Drilling Program Site 1052 in the western North Atlantic Ocean, *Mar. Micropaleontol.*, **88–89**, 41–53.
- Katz, M. E., B. S. Cramer, J. R. Toggweiler, G. Esmay, C. Liu, K. G. Miller, Y. Rosenthal, B. S. Wade, and J. D. Wright (2011), Impact of Antarctic Circumpolar Current development on late Paleogene ocean structure, *Science*, **332**, 1076–1078.
- Kennett, J. P., and N. J. Shackleton (1976), Oxygen isotopic evidence for the development of the psychrosphere 38 Myr ago, *Nature*, **260**, 513–515.
- Kennett, J. P., and P. F. Barker (1990), Latest Cretaceous to Cenozoic climate and oceanographic developments in the Weddell Sea, Antarctica: An ocean-drilling perspective, *Proc. ODP, Sci. Results*, **113**, 937–960.
- Kroopnick, P. (1985), The distribution of ^{13}C of ΣCO_2 in the world oceans, *Deep Sea Res.*, **32**, 57–84.
- Laskar, J., A. Fienga, M. Gastineau, and H. Manche (2011), La2010: A new orbital solution for the long-term motion of the Earth, *Astron. Astrophys.*, **532**, A89, doi:10.1051/0004-6361/201116836.
- Latimer, J. C., and G. M. Filippelli (2002), Eocene to Miocene terrigenous imports and export production: Geochemical evidence from ODP Leg 177, Site 1090, *Palaeogeogr. Palaeoclimatol. Palaeoecol.*, **182**, 151–164.
- Laws, E. A., P. G. Falkowski, W. O. Smith Jr., H. Ducklow, and J. J. McCarthy (2000), Temperature effects on export production the ocean, *Global Biogeochem. Cycles*, **14**, 1231–1246, doi:10.1029/1999GB001229.
- Lawver, L. A., and L. M. Gahagan (1998), Opening of Drake Passage and its impact on Cenozoic ocean circulation, in *Tectonic Boundary Conditions for Climate Reconstructions*, edited by T. J. Crowley and K. C. Burke, pp. 212–223, Oxford Univ. Press, Oxford.
- Lawver, L. A., and L. M. Gahagan (2003), Evolution of Cenozoic seaways in the circum-Antarctic region, *Palaeogeogr. Palaeoclimatol. Palaeoecol.*, **198**, 11–38.
- Lazarus, D. B., B. Kotrc, G. Wulf, and D. N. Schmidt (2009), Radiolarians decreased silicification as an evolutionary response to reduced Cenozoic ocean silica availability, *Proc. Natl. Acad. Sci. U.S.A.*, **106**(23), 9333–9338, doi:10.1073/pnas.0812979106.
- Lear, C. H., H. Elderfield, and P. A. Wilson (2003), A Cenozoic seawater Sr/Ca record from benthic foraminiferal calcite and its application in determining global weathering fluxes, *Earth Planet. Sci. Lett.*, **208**, 69–84.
- Lear, C. H., T. R. Bailey, P. N. Pearson, H. K. Coxall, and Y. Rosenthal (2008), Cooling and ice growth across the Eocene-Oligocene transition, *Geology*, **36**, 251–254, doi:10.1130/G24584A.1.
- Levin, L. A., and C. L. Thomas (1989), The influence of hydrodynamic regime on infaunal assemblages inhabiting carbonate sediments on central Pacific seamounts, *Deep-Sea Res.*, **26**(12), 1897–1915.
- Lisitzin, A. P. (1972), Distribution of siliceous microfossils in suspension and in bottom sediments, *Spec. Publ. Soc. Econ. Paleontol. Miner.*, **171**, 173–195.
- Litchman, E., C. A. Klausmeier, and K. Yoshiyama (2009), Contrasting size evolution in marine and freshwater diatoms, *Proc. Natl. Acad. Sci. U.S.A.*, **106**(8), 2665–2670, doi:10.1073/pnas.0810891106.
- Liu, Z., M. Pagani, D. Zinniker, R. DeConto, M. Huber, H. Brinkhuis, S. R. Shah, R. M. Leckie, and A. Pearson (2009), Global cooling during the Eocene-Oligocene climate transition, *Science*, **323**, 1187–1190.
- Livermore, R. A., A. Nankivell, G. Eagles, and P. Morris (2005), Paleogene opening of Drake Passage, *Earth Planet. Sci. Lett.*, **236**, 459–470.
- Livermore, R. A., C.-D. Hillenbrand, M. Meredith, and G. Eagles (2007), Drake Passage and Cenozoic climate: An open and shut case?, *Geochem. Geophys. Geosyst.*, **8**, Q01005, doi:10.1029/2005GC001224.
- Loubere, P. (1994), Quantitative estimation of surface ocean productivity and bottom water oxygen concentration using benthic foraminifera, *Paleoceanography*, **9**, 723–737, doi:10.1029/94PA01624.
- Loubere, P. (2002), Remote vs. local control of changes in eastern equatorial Pacific bioproductivity from the Last Glacial Maximum to the present, *Global Planet. Change*, **35**, 113–126.
- Lyle, M., A. Olivarez Lyle, J. Backman, and A. Tripathi (2005), Biogenic sedimentation in the Eocene equatorial Pacific—The stuttering greenhouse and Eocene carbonate compensation depth, in *Proceedings ODP, Sci. Results*, vol. 199, edited by P. A. Wilson, M. Lyle, and J. V. Firth, pp. 1–35, Ocean Drill. Program, College Station, Tex., doi:10.2973/odp.proc.sr.199.201.2005.
- Lyle, M., S. Gibbs, T. C. Moore, and D. K. Rea (2008), Late Oligocene initiation of the Antarctic Circumpolar Current: Evidence from the South Pacific, *Geology*, **35**(8), 691–694, doi:10.1130/G23806A.1.
- Misra, S., and P. N. Froelich (2012), Lithium isotope history of Cenozoic seawater: Changes in silicate weathering and reverse weathering, *Science*, **335**, 818–823.
- Moore, T. C. (2013), Erosion and reworking of Pacific sediments in the Eocene-Oligocene transition, *Paleoceanography*, **27**, 1–13, doi:10.1002/palo.20027.
- Moore, T. C., and S. Kamikuri (2012), Data report: Radiolarian stratigraphy across the Eocene/Oligocene boundary in the equatorial Pacific, Sites 1218, U1333, and U1334, in *Proceedings IODP*, vol. 320/321, edited by H. Pälike et al., Integr. Ocean Drill. Program Management International, Inc., Tokyo, doi:10.2204/iodp.proc.320321.204.2012.
- Moore, T. C., Jr. (1969), Radiolaria: Change in skeletal weight and resistance to solution, *Geol. Soc. Am. Bull.*, **80**, 2103–2108.
- Moore, T. C., Jr. (1973), Radiolaria from Leg 17 of the Deep Sea Drilling Project, in *Initial Report DSDP*, vol. 17, edited by E. Winterer et al., pp. 797–870, U.S. Government Printing Office, Wash.
- Moore, T. C., Jr., J. Backman, I. Raffi, C. Nigrini, A. Sanfilippo, H. Pälike, and M. Lyle (2004), The Paleogene tropical Pacific: Clues to circulation, productivity and plate motion, *Paleoceanography*, **19**, PA3013, doi:10.1029/2003PA000998.
- Moore, T. C., Jr., R. D. Jarrard, A. Olivarez Lyle, and M. Lyle (2008), Eocene biogenic silica accumulation rates at the Pacific equatorial divergence zone, *Paleoceanography*, **23**, PA2202, doi:10.1029/2007PA001514.
- Murray, D. W., J. W. Farrell, and V. McKenna (1995), Biogenic sedimentation at site 847, eastern equatorial Pacific ocean, during the past 3 my, in *Proceedings ODP, Science Results*, vol. 138, edited by N. G. Pisias et al., pp. 429–459, Ocean Drill. Program, College Station, Tex.
- Murray, R. W., M. Leinen, and C. W. Knowlton (2012), Links between iron input and opal deposition in the Pleistocene equatorial Pacific Ocean, *Nat. Geosci.*, **5**, 270–274.
- Nigrini, C. A., A. Sanfilippo, and T. C. Moore Jr. (2006), Cenozoic radiolarian biostratigraphy: A magnetobiostratigraphic chronology of Cenozoic sequences from ODP Sites 1218, 1219, and 1220, equatorial Pacific, in *Proceedings ODP, Sci. Results*, vol. 199, edited by P. A. Wilson, M. Lyle, and J. V. Firth, pp. 1–76, Ocean Drill. Program, College Station, Tex., doi:10.2973/odp.proc.sr.199.225.2006.
- Nielsen, E. B., L. D. Anderson, and M. L. Delaney (2003), Paleoproductivity, nutrient burial, climate change and the carbon cycle in the western equatorial Atlantic across the Eocene/Oligocene boundary, *Paleoceanography*, **18**(1), 1057, doi:10.1029/2002PA000804.
- Nong, G. T., R. G. Najjar, D. Seidov, and W. H. Peterson (2000), Simulation of ocean temperature change due to the opening of Drake Passage, *Geophys. Res. Lett.*, **27**, 2689–2692, doi:10.1029/1999GL011072.
- Olivarez Lyle, A., and M. Lyle (2006a), Organic carbon and barium in Eocene sediments: Possible controls on nutrient recycling in the Eocene equatorial Pacific Ocean, in *Proceedings ODP, Science Results*, vol. 199, edited by P. A. Wilson, M. Lyle, and J. V. Firth, pp. 1–33, Ocean Drill. Program, College Station, Tex.

- Olivarez Lyle, A., and M. W. Lyle (2002), Determination of biogenic opal in pelagic marine sediments: A simple method revisited in the Eocene equatorial Pacific Ocean, in *Proceedings ODP, Initial Results*, vol. 199, edited by P. A. Wilson, M. Lyle, and J. V. Firth, pp. 1–21, Ocean Drill Program, College Station, Tex.
- Olivarez Lyle, A., and M. W. Lyle (2006b), Missing organic carbon in Eocene marine sediments: Is metabolism the biological feedback that maintains end-member climates?, *Paleoceanography*, *21*, PA2007, doi:10.1029/2005PA001230.
- Pagani, M., M. Huber, Z. Liu, S. M. Bohaty, J. Henderiks, W. Sijp, S. Krishnan, and R. M. DeConto (2011), The role of carbon dioxide during the onset of Antarctic glaciation, *Science*, *334*, 1261–1264.
- Paillard, D., L. Labeyrie, and P. Yiou (1996), Macintosh program performs time-series analysis, *Eos Trans. AGU*, *77*, 379, doi:10.1029/96EO00259.
- Pälike, H., R. D. Norris, J. O. Herrle, P. A. Wilson, H. K. Coxall, C. H. Lear, N. J. Shackleton, A. K. Tripathi, and B. S. Wade (2006), The heartbeat of the Oligocene climate system, *Science*, *314*, 1894–1898, doi:10.1126/science.1133822.
- Pälike, H., H. Nishi, M. Lyle, I. Raffi, A. Klaus, K. Gamage, and the Expedition 320/321 Scientists (2009), Pacific Equatorial Age Transect, *IODP Prel. Rept.*, *320*, doi:10.2204/iodp.pr.320.2009.
- Pälike, H., et al. (2012), A Cenozoic record of the equatorial Pacific carbonate compensation depth, *Nature*, *488*, 609–613, doi:10.1038/nature11360.
- Parés, J. M., and T. C. Moore (2005), New evidence for the Hawaiian hotspot plume motion since the Eocene, *Earth Planet. Sci. Lett.*, *237*, 951–959.
- Paytan, A., and E. M. Griffith (2007), Marine barite: Recorder of variations in ocean export productivity, *Deep Sea Res., Part II*, *54*, 687–705, doi:10.1016/j.dsr2.2007.01.007.
- Pearson, P. N., G. L. Foster, and B. S. Wade (2009), Atmospheric carbon dioxide through the Eocene–Oligocene climate transition, *Nature*, *461*, 1110–1113, doi:10.1038/nature08447.
- Pearson, P. N. P., I. A. McMillan, B. S. Wade, T. Dunkley Jones, H. K. Coxall, P. R. Bown, and C. H. Lear (2008), Extinction and environmental change across the Eocene–Oligocene boundary in Tanzania, *Geology*, *36*(2), 179–182.
- Pfuhl, H. A., and I. N. McCave (2005), Evidence for late Oligocene establishment of the Antarctic Circumpolar Current, *Earth Planet. Sci. Lett.*, *235*, 715–728.
- Plancq, J., E. Mattioli, B. Pittet, L. Simon, and V. Grossi (2014), Productivity and sea-surface temperature changes recorded during the late Eocene–early Oligocene at DSDP Site 511 (South Atlantic), *Palaeoogeogr. Palaeoecol. Palaeoecol.*, *407*, 34–44.
- Poore, R. Z., and R. K. Matthews (1984), Late Eocene–Oligocene oxygen and carbon isotope record from South Atlantic Ocean, Deep Sea Drilling Project Site 522, in *Initial Reports DSDP*, vol. 73, edited by K. J. Hsü et al., pp. 725–735, U.S. Government Printing Office, Washington, D. C.
- Rabosky, D. L., and U. Sorhannus (2009), Diversity dynamics of marine planktonic diatoms across the Cenozoic, *Nature*, *457*, 183–186, doi:10.1038/nature07435.
- Ravizza, G., and F. Paquay (2008), Os isotope chemostratigraphy applied to organic-rich marine sediments from the Eocene–Oligocene transition on the West African margin (ODP Site 959), *Paleoceanography*, *23*, PA2204, doi:10.1029/2007PA001460.
- Salamy, K. A., and J. C. Zachos (1999), Latest Eocene–Early Oligocene climate change and Southern Ocean fertility: Inferences from sediment accumulation and stable isotope data, *Palaeoogeogr. Palaeoecol. Palaeoecol.*, *145*, 61–77, doi:10.1016/S0031-0182(98)00093-5.
- Sarmiento, J. L., N. Gruber, M. A. Brzezinski, and J. P. Dunne (2004), High-latitude controls of thermocline nutrients and low latitude biological productivity, *Nature*, *427*, 56–60.
- Scher, H. D., and E. E. Martin (2004), Circulation in the Southern Ocean during the Paleogene inferred from neodymium isotopes, *Earth Planet. Sci. Lett.*, *228*, 391–405.
- Scher, H. D., and E. E. Martin (2006), Timing and climatic consequences of the opening of the Drake Passage, *Science*, *312*, 428–430.
- Schrader, H. J., and R. Gersonde (1978), Diatoms and silicoflagellates, in *Micropaleontological Counting Methods and Techniques: An Exercise of an Eight Metres Section of the Lower Pliocene of Cap Rossello Sicily*, edited by W. J. Zachariasse et al., *Micropaleontol. Bull.*, *17*, pp. 129–176, Utrecht.
- Schumacher, S., and D. Lazarus (2004), Regional differences in pelagic productivity in the late Eocene to early Oligocene—A comparison of southern high latitudes and lower latitudes, *Palaeoogeogr. Palaeoecol. Palaeoecol.*, *214*, 243–263.
- Sijp, W. P., and M. H. England (2004), Effect of the Drake Passage throughflow on global climate, *J. Phys. Oceanogr.*, *34*, 1254–1266.
- Sijp, W. P., M. H. England, and J. R. Toggweiler (2009), Effect of ocean gateway changes under greenhouse warmth, *J. Clim.*, *22*, 6639–6652.
- Sijp, W. P., M. H. England, and M. Huber (2011), Effect of the deepening of the Tasman Gateway on the global ocean, *Paleoceanography*, *26*, PA4207, doi:10.1029/2011PA002143.
- Smetacek, V. (1999), Diatoms and the ocean carbon cycle, *Protist*, *150*, 25–32.
- Stickley, C. E., H. Brinkhuis, S. A. Schellenberg, A. Sluijs, U. Rohl, M. Fuller, M. Grauert, M. Huber, J. Warnaar, and G. L. Williams (2004), Timing and nature of the deepening of the Tasmanian Gateway, *Paleoceanography*, *19*, PA4027, doi:10.1029/2004PA001022.
- Takata, H., R. Nomura, and B.-K. Khim (2010), Response of abyssal benthic foraminifera to mid-Oligocene glacial events in the eastern Equatorial Pacific Ocean (ODP Leg 199), *Palaeoogeogr. Palaeoecol. Palaeoecol.*, *198*, 11–37.
- Thomas, E., and A. J. Gooday (1996), Cenozoic deep-sea benthic foraminifers: Tracers for changes in oceanic productivity?, *Geology*, *24*(4), 355–358.
- Toggweiler, J. R., and H. Björnsson (2000), Drake Passage and paleoclimate, *J. Quat. Sci.*, *15*, 319–328.
- Torres, M. E., H. J. Brumsack, G. Bohrmann, and K. C. Emeis (1996), Barite fronts in continental sediments: A new look at barium remobilization in the zone of sulfate reduction and formation of heavy barites in authigenic fronts, *Chem. Geol.*, *127*, 125–139.
- Van Andel, T. H. (1975), Mesozoic/Cenozoic calcite compensation depth and the global distribution of calcareous sediments, *Earth Planet. Sci. Lett.*, *26*, 187–194.
- Van der Zwaan, G. J., I. A. P. Duijnste, M. den Dulk, S. R. Ernst, N. T. Jannink, and T. J. Kouwenhoven (1999), Benthic foraminifers: Proxies or problems? A review of paleoecological concepts, *Earth Sci. Rev.*, *4*, 213–236.
- Vanden Berg, M. D., and R. D. Jarrard (2004), Cenozoic mass accumulation rates in the equatorial Pacific based on high-resolution mineralogy of Ocean Drilling Program Leg 199, *Paleoceanography*, *19*, PA2021, doi:10.1029/2003PA000928.
- Via, R. K., and D. J. Thomas (2006), Evolution of Atlantic thermohaline circulation: Early Oligocene onset of deep-water production in the North Atlantic, *Geology*, *34*, 441–444, doi:10.1130/G22545.1.
- Wade, B. S., and D. Kroon (2002), Middle Eocene regional climate instability: Evidence from the western North Atlantic, *Geology*, *30*(11), 1011–1014, doi:10.1130/0091-7613(2002)030.
- Wade, B. S., and P. N. Pearson (2008), Planktonic foraminiferal turnover, diversity fluctuations and geochemical signals across the Eocene/Oligocene boundary in Tanzania, *Mar. Micropaleontol.*, *68*, 244–255.
- Wade, B. S., W. A. Berggren, and R. K. Olsson (2007), The biostratigraphy and paleobiology of Oligocene planktonic foraminifera from the equatorial Pacific Ocean (ODP Site 1218), *Mar. Micropaleontol.*, *62*, 167–179.

- Wade, B. S., A. J. P. Houben, W. Quaijtaal, S. Schouten, Y. Rosenthal, K. G. Miller, M. E. Katz, J. D. Wright, and H. Brinkhuis (2012), Multiproxy record of abrupt sea-surface cooling across the Eocene-Oligocene transition in the Gulf of Mexico, *Geology*, *40*(2), 159–162, doi:10.1130/G32577.1.
- Weber, M. E., and N. G. Pisias (1999), Spatial and temporal distribution of biogenic carbonate and opal in deep-sea sediments from the eastern equatorial Pacific: Implications for ocean history since 1.3 Ma, *Earth Planet. Sci. Lett.*, *174*, 59–73.
- Westerhold, T., et al. (2012), Revised composite depth scales and integration of IODP Sites U1331 -U1334 and ODP Sites 1218–1220, in *Proceeding IODP*, vol. 320/321, edited by H. Pälike et al., Integr. Ocean Drill. Program Management International, Inc., Tokyo, doi:10.2204/iodp.proc.320321.201.2012.
- Westerhold, T., U. Röhl, H. Pälike, R. Wilkens, P. A. Wilson, and G. Acton (2014), Orbitally tuned time scale and astronomical forcing in the middle Eocene to early Oligocene, *Clim. Past*, *10*, 955–973, doi:10.5194/cp-10-955-2014.
- Yang, S., E. Galbraith, and J. Palter (2013), Coupled climate impacts of the Drake Passage and the Panama Seaway, *Clim. Dyn.*, *43*, 37–52, doi:10.1007/s00382-013-1809-6.
- Zachos, J. C., T. M. Quinn, and K. A. Salamy (1996), High-resolution (104 years) deep-sea foraminiferal stable isotope records of the Eocene–Oligocene climate transition, *Paleoceanography*, *11*, 251–266, doi:10.1029/96PA00571.
- Zhang, Z., Q. Yan, and H. Wang (2010), Has the Drake Passage played an essential role in the Cenozoic cooling, *Atmos. Ocean Sci. Lett.*, *3*(5), 288–292.
- Zhang, Z., K. H. Nisancioglu, F. Flatøy, M. Bentsen, I. Bethke, and I. Wang (2011), Tropical seaways played a more important role than high latitude seaways in Cenozoic cooling, *Clim. Past*, *7*, 801–813.